Support for Forest Conservation Imperatives: A Robust Approach for Multi-dimensional, Spatially Explicit Resilience Assessment

Authors: Bryan A. Fuentes[a], Patricia N. Manley[b], Nicholas A. Povak[b]

[a] Resilient Forestry, 6523 California Ave., SW, Seattle, WA 98136
[b] USDA Forest Service, Pacific Southwest Research Station, 2480 Carson Rd., Placerville, CA, USA

Corresponding author: bryanfuentes@resilientforestry.com

Key words: Composite indicator; Forest resilience; Ecosystem condition metrics; Optimized weighting; Socio-ecological resilience

Abstract

Forest ecosystems are ecologically, socially, and culturally valuable, and are arguably considered essential to global sustainability. Climate change and altered disturbance regimes are threatening the future of forests around the globe. Many countries are coming together to support and implement conservation and monitoring initiatives to improve future prospects for the restoration and persistence of resilient forest ecosystems. Policies and regulations pertaining to forest conservation require reliable and informative measures of condition and management effectiveness to sustain investments and show progress. Composite indicators provide a promising approach for quantifying forest resilience across scales, yet their development is often inconsistent, lacking theoretical rigor and sensitivity to ecological context. This study presents two transparent, scalable pathways for constructing composite indicators of ecosystem resilience, with a focus on forest resilience in California's Sierra Nevada. We operationalize the Ten Pillars of Resilience (TPOR) framework and apply two core metric selection methods: Real Core Metrics (RCM) via hierarchical clustering and Synthetic Core Metrics (SCM) via factor analysis, both combined with climate-based ecological stratification, fuzzy logic-based normalization, and optimized metric weighting. Composite indicators were developed using both compensatory and non-compensatory aggregation techniques. Results show that stratified, optimized approaches (RCM and SCM) outperformed a traditional, landscape-wide theoretical model by better capturing ecological variability and avoiding bias from outliers. The SCM approach produced more symmetric and statistically elegant indicators, while RCM indicators retained interpretability through direct ties to tangible forest attributes. We introduce an Information Retention Index (IRI) to quantify the amount of information preserved by the composite indicators and conduct a Monte Carlo-based sensitivity analysis to assess the stability of indicator outputs across methodological choices. Our pathways advance the rigor, transparency, and ecological relevance of composite indicator development, providing a robust foundation for spatially explicit resilience assessments that support adaptive management and conservation investments.

1. Introduction

Forest ecosystems provide and support a wealth of ecosystem services and their conservation has long been recognized as critical to the future of global sustainability and quality of life (Payn et al., 2023). Forests in western North America and around the globe are experiencing unprecedented stress from the confluence of climate change and altered disturbance regimes, leading to widespread concerns about their long-term resilience (Hessburg et al., 2019) and sustainability of the many critical ecosystem services (e.g., water, carbon, biodiversity, wood products) provided by forest ecosystems. Recent declarations and commitments to forest conservation, such as the Kananskis Wildfire Charter recently adopted by the G7 (Group of Seven, 2025), the Forest Monitoring Law recently adopted by the European Union (Resco De Dios and Boer, 2025), and the Global Biodiversity Framework (Burgess et al., 2024) developed by the Convention on Biodiversity all call for near-term progress (next 5 years) across multiple metrics and ecosystem facets as critically important to the future of forests and global sustainability. Concomitantly, there is an increasing growing need to identify meaningful and actionable metrics to characterize ecosystem condition, their status, and change over time toward motivating conservation investments and enhancing conservation finance mechanisms and investments (e.g., Lawler et al., 2020; Waldron et al., 2013).

Ecological resilience, the capacity of a forest to persist through, recover from, or reorganize in response to disturbance (Falk et al., 2022), is an emergent property governed by complex interactions across multiple scales. Human activities, such as fire suppression or large-scale land management, can either enhance or degrade resilience. For instance, fire-adapted ecosystems require periodic low-to-moderate intensity fires to maintain ecosystem functions, but human intervention in the form of fire suppression has contributed to a greater prevalence of high-severity fires that threaten forest resilience, as well as human life and property (Franco-Gaviria et al., 2022; Hessburg et al., 2019; Keane et al., 2018). Furthermore, it is becoming essential to consider the impacts and constraints that future climate is projected to have on landscape conditions (e.g., Povak and Manley 2024) and to inform effective investments in both near-term and long-term outcomes of importance (e.g., Bastiaansen et al., 2020; Cumming, 2011; Povak and Manley, 2024). In short, with increasing wildfire severity, drought-induced mortality, and the potential for large-scale vegetation type-conversions, there is a critical need for robust, spatially explicit methods to quantify forest resilience in a way that can effectively guide management and conservation investments (Keane et al., 2018; Forzieri et al., 2022).

Assessing the multifaceted nature of forest resilience requires an approach that can integrate the key ecological dimensions that underpin resilience, namely forest structure, composition, and disturbance dynamics (Manley et al., 2023). To this end, composite indicators offer a powerful tool for synthesizing diverse, functionally relevant metrics into a cohesive and interpretable assessment (Sharifi and Yamagata, 2016). By aggregating variables that directly measure attributes like tree density, species diversity, and fire return interval departure (Manley et al., 2023), composite indicators can provide a holistic view of resilience across vast and heterogeneous landscapes. However, the utility of such indicators is contingent on a methodologically sound and transparent construction process (Nardo et al., 2008).

Environmental conservation and assessment programs around the world are committing to: 1) understand multidimensional conditions and threats to forest resilience (Brand, 2009; De Leo and Levin, 1997); 2) quickly inform effective conservation action (e.g., Elsen et al., 2020); and 3) show measurable results to justify and motivate investment (e.g., De Groot et al., 2013; zu Ermgassen and Löfqvist, 2024). The complexity of socio-ecological systems necessitates multi-metric approaches to forest condition and management assessments to capture the multidimensional nature of resilience and its implications for providing ecosystem services (e.g., de Jonge et al., 2012; de Juan et al., 2018). However, the success of such initiatives is contingent upon the ability to adequately characterize individual metrics at high-resolution across large spatial extents (e.g., tree density), and summarize them across multiple metrics (e.g., forest structure) to make inferences about higher order conditions (e.g., forest health; McDonald and Lane, 2004) in a robust and repeatable manner. A clear pathway to quantifying status and change across multiple metrics and ecosystem facets that can be reproduced across continents and the globe is lacking.

Composite indicators are the outputs of the aggregation of multiple individual variables or metrics into a single index, which capture multi-dimensional aspects of complex phenomena (Tate, 2012). These indicators are particularly useful in comparing and ranking conditions across various domains such as the intersection of forest resilience with biodiversity conservation, carbon sequestration, water security, and economic competitiveness and prosperity over space and time (Nardo et al., 2008). Composite indicators within and among resource topic areas offer a valuable solution by integrating two or more metrics into a single value that reflects a facet of the landscape (e.g. forest resilience), that can be applied similarly across multiple facets the landscape and ideally be combined to reflect the status and change of complex ecosystems (Briguglio et al., 2009; Sharifi and Yamagata, 2016). These indicators allow for the quantification of resilience at multiple scales, offering a more holistic and comprehensive view of how systems respond to disturbances (Cutter et al., 2014). For example, the integration of ecological indicators (e.g., biodiversity, soil quality) with social factors (e.g., governance capacity, community adaptation) can provide critical insights into how resilience is distributed across landscapes and communities and the degree to which they are interdependent (Liggs et al., 2015).

Environmental composite indicators are not new, but they are largely limited to singular resource areas. Most applications have resulted in indices (spatially explicit or not) assessing the current and/or future state of a system to address specific resource outcomes, such as ecological suitability, habitat quality, hazard exposure, management opportunities, stability under climate change, and facets of social well-being tailored to particular places. Examples of such applications include the assessment of sustainability of agriculture practices (Gómez-Limón et al., 2020; Talukder et al., 2017), quality and stability of biodiversity habitats (Castro-Pardo et al., 2022; Klausmeyer et al., 2011; Riedler et al., 2015; Suraci et al., 2023; Yu et al., 2017), prioritization of forest management strategies (Brovkina et al., 2017; Lin, 2020; Marín et al., 2021; Pert, 2011; Tarasewicz and Jönsson, 2021), land use and land cover degradation (Benini et al., 2010; De Montis et al., 2020; van Oudenhoven et al., 2012), productivity of marine and coastal ecosystems (Campos et al., 2022; Yamada et al., 2021; Ye and Link, 2023),

resilience or vulnerability to environmental hazards and climate change (Ferrier et al., 2020; Flensborg et al., 2023; Hiete et al., 2012; Kotzee and Reyers, 2015; Lung et al., 2013; Salvati et al., 2013, Thakur et al., 2019), and water security (Chung and Lee, 2009; Lü and Lü, 2021; Molinos-Senante et al., 2014).

Many of the barriers to accessing and integrating high-resolution spatially explicit data into environmental applications have been removed in recent years. However, with big data can come big problems due to the "curse of dimensionality", which impacts the ability to make meaningful and actionable decisions due to the inherent complexity of the data. The crux of the issue is to find a balance between including enough information (e.g., number of individual metrics) to adequately characterize the system of interest while ensuring the analysis is easily interpretable to the large and potentially diverse end-user base. Forest conservation and land management programs remain challenged with inconsistent and potentially under performing approaches to creating composite indicators that can effectively support investment and measure progress when they are needed more than ever. In most cases, metrics are normalized (aka scored) and then those scores are simply summed or averaged, or the range of values are presented in some form (e.g., bar charts) and shifts in conditions within and among metrics are summarized (Gorman et al., 2024; Keene and Pullin, 2011). These approaches, despite their widespread use, frequently are inadequate to the task of incisively informing strategic investments in forest restoration and conservation, and the unintended bias in these approaches can make them less stable and reliable measures of condition, two fundamental requirements for bolstering market demand and financial investment (e.g., "bridging conservation funding gap", Thompson, 2023; Perino et al., 2022; Gonon et al., 2024; Clark et al., 2018).

Creating useful and reliable composite indicators is a complex process that requires careful consideration to ensure accuracy, relevance, and representation (Nardo et al., 2008). Four primary components to the development of composite indicators and their evaluation include: 1) selecting a strong theoretical framework that clearly defines the concept being represented (Booysen, 2002); 2) selecting metrics that have individual appeal but also make strong contributions to representing complex systems on the whole; 3) putting metrics on a common scale through a normalization process that does not bias their representation; and 4) summarizing conditions across metrics without losing the inherent variability among metrics in the composite representation. The importance of a theoretical framework lies in its ability to provide a coherent structure upon which the composite indicator is built. This in turn guides the selection of metrics and their respective influence (Greco et al., 2019). Without a sound theoretical foundation, the resulting composite indicator may lack validity and could mislead users regarding the true nature of the phenomenon being represented (Burgass et al., 2017; Nardo et al., 2008).

This study presents two transparent and repeatable methodological pathways for deriving robust composite indicators to represent forest ecosystem conditions in an unbiased and geospatially integrated manner using a relatively new theoretical framework for socio-ecological systems. The two methodological pathways were designed to compare and contrast the

strengths and sensitivities of the proposed pathways to core metric selection and weighting to derive composite indicators of forest resilience. We also present a novel method of characterizing the 'information capture' accomplished by a given multi-metric representation and use the method to evaluate the effectiveness of the indicators generated by each of the two methodological pathways we explore. These pathways can be adopted by and applied to multiple ecosystem facets (not limited to forest resilience) and any conservation and restoration program at any scale, making them highly versatile. Finally, we demonstrate how it can be used to address multiple ecosystem facets to make inferences about overall landscape resilience across the Sierra Nevada ecoregion (California, United States).

2. Methods

2.1 Demonstration study area

The Sierra Nevada is a large and diverse landscape, extending approximately 650 km from north to south, and ranging in elevation from 200 to 4400 m, spanning multiple vegetation zones from foothill oak woodlands to subalpine and alpine ecosystems (Fig. 1). The region is known for high levels of endemism and biological diversity, including 13,000 different plant species, 27 species of conifers, and more than 40 different vegetation associations (Sawyer et al., 2008). Although dominated by forested public lands, the Sierra Nevada has a diversity of land ownerships, ranging from National Parks to private industrial timber lands to a wide range of urban environments. Accordingly, the Sierra Nevada provides a strong test of the efficacy and performance of composite indicator methodologies.

Fig. 1 goes here

2.2 Socio-ecological system TPOR Framework

We used the Ten Pillars of Resilience Framework (TPOR Framework) as the theoretical foundation for our composite indicator work (Manley et al., 2023). The TPOR Framework integrates both social and ecological values through ten "pillars": (1) forest resilience, (2) fire dynamics, (3) fire-adapted communities, (4) carbon sequestration, (5) air quality, (6) biodiversity conservation.(7) water security, (8) wetland integrity, (9) economic diversity, and (10) social and cultural well-being. Each pillar is comprised of one or more core *elements* (e.g., forest resilience is partitioned into structure, composition, and disturbance), which in turn are described by *metrics* that represent individual components of landscape conditions, which are in turn are quantified using spatially explicit data (e.g., raster or vector data). The relationship between pillars, elements, and metrics is hierarchical (one or more metrics are nested within a given element, one or more elements are nested within a given pillar); however in application the intermediate level of organization - the 'elements' - may or may not be included in making inferences about the overall socio-ecological system. This framework has proven useful in several landscape assessments performed at various scales to inform landscape planning and management (Manley et al., 2023; Manley et al. 2025; Povak et al., 2024).

We applied our composite indicator pathways to the forest resilience pillar of the TPOR Framework and evaluated their performance. The Sierra Nevada is a heavily forested area, and reliable spatial data on a range of forest metrics are widely available. The breadth of available data and metrics on forest conditions provided a strong test of the composite indicator pathways. Finally, we demonstrated the hierarchical application of our pathways under the TPOR lens. We achieved this through a comprehensive assessment that incorporates metrics across all 10 pillars into a multi-pillar indicator of ecosystem resilience. Figure 2 shows a schematic representation of the general workflow, including the proposed pathways to build composite indicators.

Fig. 2 goes here

2.3 Forest resilience example application

Key concepts and fundamental aspects of forest resilience, including its assessment in the context of climate change and tipping points can be found elsewhere (Holling, 1973; Newton and Cantarello, 2015; Manley et al., 2023; Scheffer and Carpenter; 2003; Reyer et al., 2015). Here, the forest resilience pillar is represented by ten metrics associated with each of three elements (structure, composition, and disturbance; Table 1). Five metrics related to forest structure, including basal area, tree density, density of large trees (> 75 cm diameter at breast height (dbh)), stand density index (SDI), and canopy fractal dimension index. Three metrics related to forest composition, including the proportion of the landscape in early and late seral stages, and the density of large snags (> 75 cm dbh). And, two metrics related to disturbance, including tree mortality and the time since the last disturbance. Each of the ten metrics were evaluated to determine if they met assumptions of a normal distribution, and statistical transformation was applied to those with the highest bias associated with skewness and outliers (Table 1).

Characterizing complex systems within a decision support framework requires selecting a comprehensive set of metrics that adequately defines the study system while also considering model parsimony to ensure outputs are easily interpreted by the end users. The selection of metrics used in the current assessment reflect that compromise as the metrics described above were picked from a larger pool of remotely sensed data for the state of California. Metric selection derived from interactions among scientists, practitioners, and government and non-government interest holders to determine those metrics that best represented landscape conditions, had direct practical application for management, and were easily communicated to users. Correlation analyses were also conducted (data not shown) among the larger set of metrics to eliminate redundant metrics while forming the final set (Table 1).These metrics also aligned with several laws, charters, and initiatives that have recently been implemented within the United States and across the globe. In sum, the metrics included in the current assessment represent not only a bottom-up approach where selection was driven by regional scientific knowledge and community engagement, but also addresses larger national and global imperatives to address the social and ecological resilience at larger scales.

Table 1 goes here

2.4 Pathways for constructing composite indicators

We explored two complementary pathways for constructing composite indicators of socio-ecological resilience (cluster analysis and factor analysis), and then demonstrated their application to forest resilience. These pathways have different strengths and sensitivities that are determined in part by the breadth and substance of metric representation, but also determined by the character of individual metrics and their relationship to one another. The selection process reflects a balance between data availability with the need to accurately represent the target phenomenon. The aim is to ensure that the chosen metrics effectively capture the multidimensional aspects of the ecosystem component or overall ecosystem. Accordingly, metrics should be selected based on their relevance to the theoretical framework and their contribution to the information presented through the composite indicator (Booysen, 2002; Dale and Beyeler, 2001; Freudenberg, 2003; Li et al., 2012).

We could have constrained the aggregation process for the forest resilience pillar to each level of the TPOR hierarchy - first aggregating metrics to their associated element, and then aggregating the three elements to the pillar (Fig. 3) - but we chose to bypass elements and aggregate all the metrics to represent the pillar. We bypassed elements in our analysis for two reasons: 1) working with a greater number of metrics provided a more robust comparison of the performance of each pathway, and 2) it was an opportunity to directly compare the outputs of these pathways to the outputs of the TPOR Framework as the theoretical foundation.

Fig. 3 goes here

2.4.1 Real Core Metric pathway

The first pathway is most applicable when few, possibly interrelated metrics are available, when the overall dimension encompassed by these metrics is not large enough to be subject to the derivation of a synthetic representation of metrics (as described in 2.4.2), or when the application calls for metrics based on real measured or estimated values (e.g., trees per unit area) such as for policy or regulatory purposes. This pathway is based on the Item Cluster Analysis (ICLUST) technique proposed by Revelle (1979). The ICLUST is a hierarchical clustering algorithm designed to group metrics into functionally homogeneous and reliable clusters. The algorithm groups metrics iteratively based on a measure of cluster homogeneity and "general factor saturation" known as Coefficient Beta (β). The coefficient β is formally defined as the worst possible split-half reliability of a cluster. Conceptually, this acts as a "stress test" for a cluster's cohesiveness. To find β, ICLUST temporarily partitions the metrics within a potential cluster into two sub-groups (i.e., halves) and finds the split that makes these two halves as statistically dissimilar as possible (by minimizing the covariance between them). If the cluster is truly homogenous, then even in this worst-case split, a strong relationship between the two halves will remain. Equation 1 shows the calculation of β for a cluster split into halves A and B of size n and m, respectively.

$$\beta = \frac{(n+m)^2 \bar{\sigma ij}'}{\sigma^2_{(A+B)}}$$

where $\bar{\sigma ij}'$ is the average between-half covariance that is minimized through cluster splitting. In its basic form, ICLUST begins with each metric as an individual cluster and proceeds iteratively. At each step, the algorithm identifies the two most correlated clusters as candidates for a merge. It then calculates the *β* of the potential new cluster. The algorithm performs the single merge that yields the largest increase in *β* and repeats the process until no further merges increase *β*, at which point the final cluster solution is reached. The function *ICLUST* of the R package *psych* (Revelle, 2025) was used to perform the metric clustering. Note that this function also uses a coefficient Alpha (α) when evaluating a potential cluster. Specific details about α and its use by ICLUST can be found in Revelle (1979) and Revelle (2025). Overall, we argue that the ICLUST technique is effective for metric reduction and/or summary for small numbers of metrics because it groups metrics into clusters based on the correlations among metrics, allowing the identification of subsets of metrics that are both internally consistent and relatively independent. By using α and *β* as a clustering criterion, the method ensures that only clusters with strong internal homogeneity are formed. This helps to select the most representative metric(s) within each cluster for subsequent analysis. We refer to this pathway and its cluster-wise selected metrics as *real core metrics* (RCM).

2.4.2 Synthetic Core Metric pathway

The second pathway is based on factor analysis (FA), and it is proposed for those scenarios where a large number of (interrelated) metrics are initially available. FA is a multivariate statistical technique commonly used to reduce the dimensionality of a set of observed metrics by identifying a smaller number of unobserved latent factors that explain the correlations among them. In the context of composite indicator analysis, FA serves as a tool to extract the underlying structure of the data, simplifying complex, high-dimensional metrics into interpretable synthetic indicators. FA operates on the principle that the observed metrics (*X*) are linear combinations of common factors (*F*) and unique variance (*E*), expressed by the fundamental model (Eq. 2):

$$X_j = \sum_{k=1}^{p} l_{jk} F_k + E_j$$

where l_{jk} represents the factor loading of the *j*-th metric on the *k*-th factor. The goal is then to identify a set of factors that effectively reproduces the original correlation structure, allowing for a parsimonious interpretation of the data's underlying dimensions. In general terms, the FA procedure begins with the variable correlation matrix (*R*), which is then decomposed to find a factor loading matrix (*L*) that best reconstructs *R* (i.e., $R \approx LL'$). The extraction of factors is guided by their eigenvalues ($\lambda_k = \sum_j l^2_{jk}$), which represent the amount of variance explained by each factor. Typically, only factors with eigenvalues greater than one are retained. The proportion of each variable's variance explained by these retained factors is its *communality* (

$h^{2_j}=\sum_k l^2{}_{jk}$). To enhance interpretability, the initial loading matrix *L* is often subjected to an orthogonal or oblique rotation (e.g., Varimax). This process achieves a "simple structure" where each variable loads strongly on only one factor, clarifying the meaning of the underlying constructs without altering the overall variance explained. This pathway assumes that the latent factors represent underlying, interpretable constructs of some aspect of socio-ecological conditions (forest resilience in our application). Furthermore, we argue that these factors are able to retain only the most relevant, non-redundant information that drives the variability in the initial pool of metrics. We refer to these latent factors as *synthetic core metrics*. The R package *psych* (Revelle, 2025) was used to conduct FA with estimation of the optimal number of factors via random parallel simulation. We refer to this pathway and its selected metrics as *synthetic core metrics* (SCM).

2.5 Metric normalization and landscape stratification

The numerical representation of the metrics selected to create a composite indicator must be normalized to ensure comparability across different units of measurement (Mazziotta and Pareto, 2016). Normalization is the means by which original or transformed (e.g., log-transformed) values of a metric are converted to a uniform range (Wang and Cumming, 2011), which for this study was set from 0 to 1. Normalization facilitates the aggregation of data that would otherwise be inherently incomparable. Without normalization, adding together metrics measured in different units would result in a composite indicator that is difficult to interpret and potentially misleading (Nardo et al., 2008). A normalization process is also needed for applications that evaluate the conditions based on targeted outcomes, which requires users to score conditions based on an a priori notion of “favorable” or “unfavorable” values expressed by a given metric (Czucz et al., 2021).

2.5.1 Normalization approaches

Although necessary in the context of developing composite indicators, normalization of spatially explicit metrics across large spatial extents and/or heterogeneous landscapes should be approached with caution. Normalization of metric values without an ecological context can limit the effectiveness of a composite indicator in accounting for regionalized, intrinsic ecological productivity and other sources of variance in ecological potential. The most commonly used normalization and standardization methods rely on the observed range and distribution of metric values as the basis for scoring, such as scaling by Z-score (mean of zero and a standard deviation of one) and min-max scaling (min set to zero, max set to one). The min-max method is popular because it preserves the relationships among indicators and is easy to interpret (Brunet, 2002). However, both min-max and Z-score normalization methods are sensitive to outliers, leading to biased or skewed composite indicators (Tarasewicz and Jönsson, 2021). Furthermore, any normalization approach that is influenced by the range and distribution of values implicitly imposes the full range of values across all sites, however biophysical constraints affect the potential range of values, and the resulting extreme values and outliers can lead to skewed scores and reduced variability of metric values across the landscape (Tarasewicz and Jönsson, 2021).

The reference values method can be independent of the existing range and distribution of values, as they are user-defined scores based on proximity to one or more reference values (aka, target values) (El Gibari et al., 2018; Saisana and Saltelli, 2011; Talukder et al., 2017). The proximity measure can be constrained to a specific range outside of which proximity values immediately become (e.g.) zero or one. Moreover, the proximity measure can be forced to follow certain mathematical functions, which result in this measure having a particular 'shape'. Some of the mathematical functions commonly used to score metrics using reference values are the membership functions (MF), which are widely applied in fuzzy logic. Fuzzy logic, originally introduced by Lotfi Zadeh in 1965, is a mathematical framework for dealing with uncertainty and vagueness (Zadeh, 1965). Fuzzy logic extends classical binary logic (true/false) by allowing variables to have a degree of truth ranging between 0 and 1. This feature makes fuzzy logic particularly suitable for situations where precise boundaries between ranks, classes, or categories are difficult to define (Zani et al., 2013).

In the context of composite indicators, a MF maps a given metric into a continuous space where the proximity of each metric value to one or more reference values is quantified. The number and interpretation of reference values dictates the shape of membership function to use, and thus, the parametrization (Munda, 1995). Examples of these functions include the following: (i) s-shaped function (increases from 0 to 1 between the reference values x and y); (ii) z-shaped function (decreases from 0 to 1 between the reference values x and y); (iii) triangular function (increases from 0 to 1 between x and y, and then decreases from 1 to 0 between y and z); (iv) trapezoidal function (similar to triangular function but with a flat top achieved by including a fourth reference value); and, (v) non-linear variants of these functions based on Gaussian and sigmoid curves (Iliadis et al., 2010). A "higher is better", "lower is better", etc., reasoning of reference values is commonly used to select the shape and parametrization of membership functions to score metrics (Kouikoglou and Phillis, 2011).

2.5.2 Climate-based strata

For our application, we addressed the ecological context for normalization by 1) creating climate-based ecological strata across the Sierra Nevada to reflect variability in biophysical constraints by geographic zones (Povak and Fuentes., *in press*; Fig. 4), and 2) using a combination of range-based and reference-based metric interpretations for normalization and weighting. We followed an ecological stratification approach based on climate characteristics, similar to the one proposed by Jeronimo et al. (2019). These authors based their approach on the climate analogs concept (Churchill et al., 2013) to cluster climatic variables into climate strata. We used the Basin Characterization Model (BCM) (Flint et al., 2021) dataset to construct 30-year normals (1981-2010) of actual evapotranspiration (AET), climatic water deficit (CWD), minimum annual temperature (Tmin), and maximum annual temperature (TMax). We selected these variables as representatives of biophysical factors that affect vegetation productivity, moisture stress, regeneration and growth (Dobrowski et al., 2013; Jeronimo et al., 2019; Lutz et al., 2010).

Fig. 4 goes here

The climate strata were created by agglomerative nesting (i.e., hierarchical clustering) of the climate variables based on the Ward method. We evaluated the clustering dendrogram, the corresponding scree plot, and the silhouette index (Rousseeuw, 1987) to select the optimal number of climate strata. The cluster analysis resulted in five climate strata (Povak and Fuentes., *in press*) that generally conformed to elevation bands along the western slope of the Sierra Nevada (Fig. 4; see section 3.5 for more details). We conducted a PERMANOVA to test the significance of the resulting climate strata. Hierarchical clustering requires a pairwise distance matrix, which can become computationally prohibitive as the number of observations increases. Consequently, we performed stratified random sampling based on the multivariate joint distribution to select a representative subset of observations from the variables. The C5.0 algorithm (Kuhn and Quinlan, 2025) was used to project the discrete cluster assignments (i.e., climate strata) from the sampled data points back onto the entire continuous raster landscape. The model was trained using the sampled dataset where the four climate variables (AET, CWD, TMin, TMax) served as the predictor variables and the resulting stratum ID served as the categorical response variable. The cluster analysis, PERMANOVA, and C5.0 modeling were conducted in R using the packages cluster (Maerchler et al., 2025), vegan (Oksanen et al., 2025), and C50 (Kuhn and Quinlan, 2025), respectively. The R package terra (Hijmans, 2025) was used as the backend of spatial analysis including data interoperability (e.g., conversion of spatial rasters to numerical matrices and vice versa).

2.5.3 Normalization by climate strata

The normalization of metric values for multi-metric aggregation was performed by climate strata, and first entailed the elimination of outliers and the identification of endpoint values based on the remaining range of values across the climate stratum. The endpoint values were selected based on univariate outlier detection. The R package univOutl (D' Orazio, 2022) was used to detect outliers based on the following equation (Eq. 3):

$$S_{\text{left}} = \left(P\,50th - P\,10th\right)/1.2816\,;\, S_{\text{right}} = \left(P\,90th - P\,50th\right)/1.2816$$

where S_{left} and S_{right} are robust scale estimates based on percentiles (10th, 50th, and 90th) that account for skewness at both tails of the distribution. Note that if no outliers were found, the corresponding minimum or maximum value was used as the endpoint value.

The metric normalization then followed a reference value approach (El Gibari et al., 2018; Saisana and Saltelli, 2011; Talukder et al., 2017) coupled with a priori notions of "favorable" and "unfavorable" metric conditions (Czucz et al., 2021) (Table 1, Fig. 5). The endpoint values served as reference values, and the proximity measure was based on fuzzy membership. The a priori notion of a metric guided the selection of the membership function. For instance, if the a priori notion of a metric was "higher is more favorable", a linear s-shaped membership function was selected. Conversely, if the a priori notion of a metric was "lower is more favorable" a linear z-shaped function was selected. The endpoint values were used to parametrize the fuzzy membership function for a given metric within a given stratum. The equations of the linear s-

shaped (a) and the linear z-shaped (b) membership functions are shown below (Eq. 4 and Eq. 5, respectively).

$$f(x, E_1, E_2) = \begin{cases} 0 & \text{for } x < E_1 \\ \dfrac{x - E_1}{E_2 - E_1} & \text{for } E_1 \le x \le E_2 \\ 1 & \text{for } x > E_2 \end{cases}$$

$$f(x, E_1, E_2) = \begin{cases} 1 & \text{for } x < E_1 \\ \dfrac{E_2 - x}{E_2 - E_1} & \text{for } E_1 \le x \le E_2 \\ 0 & \text{for } x > E_2 \end{cases}$$

where *x* is the metric value for a given raster cell, E_1 is the lower endpoint value, and E_2 is the upper endpoint value.

Fig. 5 goes here

2.6 Weighting and aggregation

The aggregation process involves combining the individually normalized metrics into a single composite indicator. The aggregation of normalized metrics into a composite indicator includes two critical steps: (a) the definition of a weighting scheme, and (b) the selection of an aggregation function. The choices made for these two steps determine the relative influence each metric will have on the composite indicator score, and consequently the interpretations and management implications drawn from it (Becker et al., 2017). If aggregation is done at multiple levels of an information hierarchy (e.g., metrics to element, elements to pillar, pillars to ecosystem) and/or spatial scales (e.g., pixels to sub-watershed, subwatersheds to watershed, watersheds to landscape), these steps will apply to each aggregation, ideally using a consistent approach across the hierarchy.

2.6.1 Weighting scheme

Weights can be assigned to metrics based on various criteria, such as ecological importance, management objectives, policy relevance, or simply to reach a more equitable degree of influence among metrics (Gan et al., 2017, Suraci et al., 2023). As such, it is important to explicitly address how metrics are weighted (intentionally or otherwise) in aggregation. Some examples of weighting schemes include: (i) equal (“naive”) weighting, (ii) analytic hierarchical process (AHP), (iii) statistical weighting, and (iv) optimized weighting. These weighting schemes are discussed next.

Intuitively, the aggregation of normalized metrics using equal weights (i.e., no assigned weight) would lead to a balanced representation of metric variability by the final composite indicator (Suraci et al., 2023). However, distributional properties like outliers, skewness, and metric inter-correlation can cause certain metrics to have a stronger influence on the composite indicator (Becker et al., 2017; Paruolo et al., 2012; Suraci et al., 2023). The AHP for weighting usually involves the systematic, pairwise comparison of metrics to determine relative importance (Singh et al., 2007). This process is useful when empirical data support the assignment of weights, but it becomes complex as the number of metrics increases (Gan et al., 2017). Statistical weighting uses techniques like PCA and FA to assign weights proportionally to the amount of variance that a metric explains for a given component or factor (i.e., component or factor loadings). This scheme can help reveal the underlying structure of the data (Paruolo et al., 2012). However, weights derived through PCA and FA might reflect statistical properties of the data rather than the true importance of each metric according to the theoretical framework as the conceptual basis for composite indicator analysis (Hermans et al., 2008). In contrast, optimized weighting is intended to balance the influence of metrics on the composite indicator. Optimized weighting is particularly valuable when subsets of metrics are correlated, effectively reinforcing each other, which leads to an implicit increase in their combined weight (Becker et al., 2017). Additionally, metrics with higher variance, more extreme values (e.g., a skewed distribution), or metrics normalized using larger ranges, can have a disproportionate impact on the composite score, even if all metrics are equally weighted (Nardo et al., 2008).

We adopted a modified version of the indicator-weight optimization method proposed by Becker et al. (2017), which serves to equilibrate the influence each metric has on the aggregated composite score. While Becker et al. (2017) optimized weights using a nonlinear Pearson correlation ratio estimated via Gaussian Processes and penalized splines, our approach was based on the proportion of variance explained by each metric, derived from fitting Generalized Additive Models (GAMs; Wood, 2017) with thin plate regression splines. Specifically, for each metric, we fit a separate GAM with the composite indicator as the response and the given metric as the predictor. The variance explained by each GAM served as our measure of metric importance, ensuring robustness against assumptions of linearity. We optimized metric weights using the Nelder-Mead simplex optimization algorithm (Nelder and Mead, 1965). This derivative-free numerical optimization approach iteratively adjusts metric weights to maximize the alignment between the desired and actual metric influence (denoted by the explained variance) within the composite indicator. The algorithm repeatedly evaluates different weight combinations, progressively converging toward the optimal solution that equalizes the explained variance of the composite indicator by the metrics after weighting. This approach alters the weight (decreasing or increasing) of a particular metric in order to balance the influence of all metrics on the composite indicator.

2.6.2 Aggregation method

Several aggregation functions have been proposed in the literature depending on the conceptual reasoning of the composite problem, i.e., compensatory versus non-compensatory (Greco et al., 2019; Munda, 2005). The difference between these two types of reasoning is that

559 the former assumes that a higher score on one metric can offset a low score on another (Munda
560 and Nardo, 2009). This assumption may not be appropriate when metrics represent
561 fundamentally different dimensions that should not offset each other. The most common
562 compensatory aggregation function is the linear aggregation of metrics, which is equivalent to a
563 weighted average when the sum of the metric weights is not equal to one, or to a weighted sum
564 when the sum of the weights is equal to 1 (Saisana and Tarantola, 2002). The geometric mean
565 is a non-compensatory alternative to linear aggregation (Burgass et al., 2017; Van Puyenbroeck
566 and Rogge, 2017). In the geometric mean, metrics are multiplied after being raised to the power
567 of their corresponding weight. If the sum of the weights is not equal to one, the final product is
568 rescaled by raising it to the power of the inverse of the sum of the weights (Ebert and Welsch,
569 2004).
570
571 For each pathway, we explored two mathematical approaches to combining metrics once their
572 weights were optimized to derive the final composite indicator: (a) compensatory, and (b) non-
573 compensatory. The compensatory aggregation was based on the weighted arithmetic mean,
574 calculated as (Eq. 6):
575

576 $$C_a = \sum_{i=1}^{n} \left(w_i x_i \right)$$

577
578 where C_a represents the compensatory composite indicator score, x_i is the normalized value of
579 the *i*-th metric (i.e., the metric score), and w_i denotes the optimized weight assigned to each
580 metric, with the sum of the weights being equal to 1. This arithmetic approach averages values
581 among metrics, thereby enabling high values for one metric to compensate for low values in
582 another in the aggregated composite indicator score. In contrast, the non-compensatory
583 aggregation was based on the weighted geometric mean, defined as (Eq. 7):
584

585 $$C_g = \prod_{i=1}^{n} \left(x_i^{w_i} \right)$$

586
587 where C_g represents the non-compensatory composite indicator score, x_i is the normalized
588 value of the *i*-th metric (i.e., the metric score), and w_i denotes the optimized weight assigned to
589 each metric, with the sum of the weights being equal to 1. This geometric approach reduces the
590 compensation among metrics, significantly penalizing composite indicator scores when one or
591 more metrics have low values, thereby inferring that the aggregate composite indicator is only
592 as strong as its weakest member, and emphasizing balance (i.e., evenness) across metrics. It is
593 important to note that the selection of endpoint conditions, normalization, weighting and
594 aggregation was performed independently for each climate stratum. This stratified approach
595 explicitly incorporates local biophysical constraints, and thereby the resulting value of the
596 composite resilience indicator reflects the intrinsic ecological productivity across the landscape
597 of interest.
598
599

2.7 Composite indicator performance

2.7.1 Information Retention Index

The practical utility of composite indicators depends on their ability to accurately represent the dimensions of the phenomenon it seeks to measure. A composite indicator without a sound theoretical framework risks being a misleading abstraction, detached from the actual state of the phenomenon it is meant to represent. In the context of our forest resilience composite indicator, this means the final score is only as meaningful as its ability to reflect the underlying ecological axes of forest structure, composition, and disturbance dynamics. The process of metric selection is therefore not a mere technical step of dimensionality reduction but is a critical stage in ensuring the indicator's ecological representativeness. Accordingly, We developed an information retention index (IRI) to quantitatively assess how much information from each individual metric is preserved by the selected core metrics (RCM or SCM). The IRI is based on the coefficient of determination (R^2) between each core metric and every other metric in the initial pool, weighted by the variance of those initial metrics. Higher IRI values suggest a more effective preservation of the original information and it provides a quantitative way to evaluate the trade-off between the RCM and SCM pathways in terms of metric representation. The statistical outline to calculate the IRI is presented below.

Let the initial pool of metrics be a set *X* with *n* individual metrics (Eq. 8):

$$X = \{X_1, X_2, \ldots, X_j, \ldots, X_n\}$$

Let the selected subset of core metrics (from either the RCM or SCM pathway) be a set *C* with *p* core metrics (Eq. 9):

$$C = \{C_1, C_2, \ldots, C_k, \ldots, C_p\}$$

First, compute the total variance of the original dataset by summing the individual variances of all *n* initial metrics (Eq. 10). This value represents the total amount of information available to be explained.

$$Var_{total} = \sum_{j=1}^{n} Var\left(X_j\right)$$

Next, for each individual core metric C_k in the selected subset *C*, calculate its specific IRI. This is done by quantifying how much of the total variance (Var_{total}) is explained by this single core metric. This is achieved by summing the variance-weighted coefficients of determination between C_k and every initial metric X_j. The formula for the IRI of a single core metric C_k is (Eq. 11):

$$IRI_k = \frac{\sum_{j=1}^{n} \left[R^2(C_k, X_j) \cdot Var(X_j) \right] * 100}{Var_{total}}$$

where $R^2(C_k, X_j)$ is the coefficient of determination (the squared Pearson correlation coefficient) between the core metric C_k and the initial metric X_j, and $Var(X_j)$ is the variance of the initial metric X_j. Finally, the overall IRI for the entire selection pathway (RCM or SCM) is calculated by taking the average of the individual IRI values for all *p* core metrics in the pathway (Eq. 12):

$$IRI_{pathway} = \frac{1}{p} \sum_{k=1}^{p} IRI_k$$

This final value represents the average proportion of total information from the initial pool of metrics that is retained by the selected set of core metrics, providing a single, quantitative measure of the pathway's representativeness. The calculation of the IRI for each pathway was made spatially-explicit by calculating its focal values using a wall-to-wall moving window. Specifically, for a given cell in the output raster layer (i.e., the focal cell), the IRI value was calculated using a square neighborhood of 9-by-9 cells centered on the focal cell. The core metrics and the initial pool of metrics were resampled from 30-meter to 300-meter cell size to make the IRI calculation computationally feasible across the study area.

2.7.2 Sensitivity analysis

The process to construct composite indicators involves a series of decisions, such as the selection of input metrics, scoring function and reference values, weighting scheme, and aggregation reasoning. Consequently, the sensitivity of a composite indicator to these methodological criteria is often quantified to assess its reliability and stability. Sensitivity analysis based on techniques like Sobol indices, coupled with resampling techniques like bootstrapping, can be used to elucidate the contribution of each criterion (e.g., reference values, weights, aggregation method) to the overall variance in the composite indicator (Saisana and Tarantola, 2002). Sensitivity analysis is particularly important in non-compensatory composite indicators, where poor performance in one dimension cannot be offset by good performance in another (Munda and Nardo, 2009; Munda and Saisana, 2011).

We conducted a comprehensive sensitivity analysis using the COINr package in R (Becker et al, 2022) to assess the robustness of our forest resilience composite indicator to methodological choices. Specifically, we evaluated the sensitivity of our composite scores to variations in three critical criteria: (1) the position of lower and upper endpoint values along the full range of metric values, (2) the balance (or lack thereof) of normalized metric weights for aggregation, and (3) the aggregation method (compensatory arithmetic mean vs. non-compensatory geometric mean). For each of these methodological components, we defined discrete alternative scenarios within COINr sensitivity analysis framework. We performed Monte Carlo simulations (N = 1000 iterations) to systematically vary these methodological criteria and quantified their impact on the

composite indicator scores. The sensitivity analysis was aimed at providing uncertainty ranges and global sensitivity indices, highlighting the manner and degree that each criterion influenced the composite indicator scores and performance. A detailed explanation of the sensitivity analysis framework adopted by COINr can be found in Saisana et al. (2005).

3. Results

3.1 Core metric selection and assignment of normalization function

3.1.1 Real Core Metrics

The item cluster analysis (ICLUST) suggested 3 clusters of correlated metrics (Fig. 6), roughly equivalent to the Disturbance, Composition, and Structure elements of the forest resilience pillar in the TPOR framework (Fig. 3). The first cluster was disturbance centric and included the metrics Time since Last Disturbance (TSD), Early Seral Stage (eSE), and Tree Mortality (Mort). The metric-composite Pearson's correlation coefficient (*r*) had the same magnitude for these 3 metrics (*r* = 0.43), but it was positive for TSD and negative for eSE and Mort. The second cluster was composition centric and included the metrics Late Seral Stage (lSE) and Snags > 40'' dbh (101.6 cm) (Snag40), which were both positively correlated with their composite (*r* = 0.73). The third cluster was structure centric and included the metrics Fractal Dimension Index of Vegetation Cover (FDI), Reineke's Stand Density Index (SDI) (Reineke, 1933), Basal Area (BA), Trees per Acre (TPA), and Trees > 30" dbh (76.2 cm) per Acre (TPA30). Overall, high metric intercorrelation in this subset resulted in higher metric-composite correlation as compared to the other cluster. The high metric intercorrelation was expected since metrics like SDI are formulated as the outputs of equations that include other metrics as parameters (Reineke, 1933; Curtis and Marshall, 2000). All the metric-composite correlations in this subset were positive, except for FDI. Figure 6 shows the result of the ICLUST, including the metric-composite correlation coefficients.

Fig. 6 goes here

The metrics eSE, Snag40, and SDI were selected as real core metrics from cluster 1, 2, and 3, respectively (Fig. 6). These metrics were selected as core metrics based on the following criteria: (a) their suitability for composite analysis (e.g., eSE is a continuous variable whereas TSD is discrete), (b) their inherent composite nature (e.g., SDI is calculated using the quadratic mean diameter and TPA, with the former being calculated using the quotient of BA and TPA), and (c) their uniqueness considering direct or inverse relationships with metrics from other clusters (e.g., Snag40 being preferred over lSE since lSE and eSE were part of the same compositional variable). A normalization function was assigned to each real core metric based on its metric-composite correlation direction (negative vs positive) within its cluster, and based on the interpretation of its cluster. A linear s-shaped function was selected as normalization function for Snag40, while a linear z-shaped membership function was assigned to SDI and eSE. The metric-composite correlation of Snag40 was positive, and its cluster was considered as representative of stable phases of vegetation succession, which are characterized by the co-

occurrence of large trees and large woody debris (both desirable indicators of forest composition) (Barry et al., 2017). The core metric SDI was positively correlated with its cluster, which was considered representative of highly dense and homogeneous structural conditions. These conditions were deemed as undesirable given the importance of structural complexity for forest resilience (Felipe-Lucia et al., 2018, Reich et al., 2021). The correlation between the core metric eSE and its cluster was negative, but the conditions represented by such cluster were deemed as desirable. This cluster was considered as representative of recovery processes mainly driven by time after disturbance events and successful tree recruitment (Sturtevant et al., 2014).

3.1.2 Synthetic Core Metrics

The factor analysis coupled with random parallel simulation suggested including three factors (i.e., synthetic metrics) to represent the dimensionality of the input metrics (Fig. 7). Good agreement was again found between the full hierarchy of the TPOR framework for the forest resilience pillar (metric-element-pillar linkages; Fig. 3) and the factors (i.e., synthetic core metrics derived from the factor analysis) (Fig. 7). The first synthetic metric (Synth1) was structure centric, being heavily loaded by metrics related to forest density and complexity, including SDI (loading = 0.86), BA (0.79), and TPA (0.78), with a strong negative loading from the FDI (0.64). This factor was interpreted as a gradient towards forest density and structural simplicity, which suggested a linear z-shaped membership function as adequate for normalization. The second synthetic metric (Synth2) was composition centric, defined by high positive loadings from metrics indicative of mature forest characteristics, namely Snag40 (0.76), TPA30 (0.75), and lSE (0.68), representing a late-successional and old-growth dimension. The third synthetic metric (Synth3) was disturbance centric, with moderate loadings from TSD (0.39) and a negative loading from eSE (-0.50), capturing a dimension of post-disturbance recovery. A linear s-shaped membership function was assigned for the normalization of these two synthetic metrics given the overall desirability of their greater values.

Fig. 7 goes here

3.1.3 Correspondence between real and synthetic core metrics

Overall, the ecological dimensions elucidated by the factor analysis corroborated the groupings identified through the ICLUST technique. Both statistical methods independently converged on the same fundamental data structures, which aligned with our theoretical TPOR framework elements of Disturbance, Composition, and Structure. In both analyses, the Structure groupings captured the greatest variation in conditions across the Sierra Nevada, followed by the Composition groupings, and with Disturbance capturing the least variation across the ecoregion. This convergence provided robust, multi-faceted evidence for the underlying relationships between the metrics and validated the selection of eSE, Snag40, and SDI as the real core metrics that effectively represent these distinct ecological dimensions.

769 **3.2 Landscape stratification and normalization**
770
771 3.2.1 Climate-based strata
772
773 Our next step after the metric selection was to stratify the Sierra Nevada landscape into distinct
774 biophysical regions to serve as the basis for developing our composite indicator. The
775 hierarchical clustering of four key climate variables - actual evapotranspiration (AET), climatic
776 water deficit (CWD), and minimum and maximum annual temperatures (Tmin, Tmax) - produced
777 five distinct climate-based strata (Fig. 8). We evaluated these strata based on the within-stratum
778 distribution of the climate variables and built the following interpretation:
779
780 Climate Stratum 1 represents the coldest environments, mainly located in high-elevation areas.
781 This stratum has the lowest median minimum and maximum temperatures (TMin = -1.6°C;
782 TMax = 12.5°C), but it still experiences notable seasonal water stress (Median CWD = 470.6
783 mm). Climate Stratum 2 is interpreted as a transitional, mid-elevation stratum. This stratum has
784 warmer temperatures than Stratum 1 (Median TMax = 15.4°C) and higher water stress (Median
785 CWD = 508.8 mm). Productivity in Stratum 2 remains high (Median AET = 412.7 mm). Climate
786 Stratum 3 shows a mix of cool temperatures similar to Stratum 2 (Median TMax = 16.1°C) with a
787 significantly higher climatic water deficit (Median CWD = 666.9 mm). These conditions may
788 explain the much lower productivity (Median AET = 222.7 mm) across this stratum. Climate
789 Stratum 4 is characterized by warm temperatures (Median TMax = 20.9°C) and the highest
790 productivity of all strata (Median AET = 488.1 mm). Water deficit is the second highest across
791 all strata (Median CWD = 706.7 mm), but water may still be available enough to support the
792 high productivity. Lastly, Climate Stratum 5 represents the most extreme conditions. This
793 stratum is defined by the highest maximum temperatures (Median TMax = 23.2°C) and the most
794 severe climatic water deficit (Median CWD = 993.1 mm). Consequently, it has very low
795 productivity (Median AET = 338.5 mm) compared to the similarly warm Stratum 4.
796
797 Fig. 8 goes here
798
799 A subsequent PERMANOVA test confirmed that these 5 climate strata were statistically
800 significant ($F=3810.62$, $p<0.001$) and explained a substantial portion of the climatic variance
801 across the study area ($R^2=0.75$) (Fig. 8). The high degree of statistical significance and the large
802 amount of variance explained validated the value of using a climate-based stratification
803 approach to selecting endpoints for normalization. It also demonstrated that the landscape could
804 be effectively partitioned into ecologically meaningful regions based on variables that govern
805 primary productivity, moisture stress, and vegetation growth. This robust, data-driven
806 stratification provided a strong biophysical template that potentially minimized the unintentional
807 bias in the normalization and weighting phases of composite indicator construction. By tailoring
808 the subsequent normalization and weighting of metrics to the specific constraints and potential
809 of these distinct regions, our approach was aligned with calls for adaptive management
810 strategies that are spatially explicit and responsive to local conditions.
811
812

3.2.2 Endpoint selection for normalization

Following the selection of core metrics and landscape stratification, our next step was to normalize the metric data in a way to make their distributions free from outliers and sensitive to regional ecological differences. (Tables S1 and S2). Within the climate strata, the distributions for eSE and Snag40 were highly skewed and leptokurtic. These non-normal distributions, characterized by extreme outliers, confirmed that a standard normalization would cause the vast majority of data points to be compressed into a small portion of the 0-1 range, disproportionately weighting the rare, extreme values. Removing outliers prior to data normalization mitigated this issue, ensuring that the fuzzy membership functions were parameterized based on the effective and most common range of values for each metric. This allowed for a more stable and representative indicator and validated the landscape stratification.

The endpoint values selected for each core metric varied significantly across the climate strata, reflecting different intrinsic ecological potentials (Fig. 9). For instance, the upper endpoint for real core metric Snag40 was 0.70 in the cool-moist-high Stratum 1, but was -0.68 in the hot-dry-low Stratum 5, indicating a fundamentally different expectation for the presence of large snags (Table S1). Similarly, the upper endpoint for eSE ranged from 0.35 in Stratum 1 to 0.60 in Stratum 3 (Table S1). This variability demonstrated that a single, landscape-wide normalization scheme would have failed to capture the unique ecological context of each region for at least some metrics. By constraining the normalization process to stratum-specific endpoint values, the resulting composite indicator evaluates conditions relative to a local baseline, making it a more precise and ecologically defensible tool for informing management. Table S1 shows summary statistics of the real core metrics and their endpoint values selected through the outlier-detection approach. Figure 9 shows boxplots with quantile marks and the region within the endpoint values to denote the metrics distribution and outlier-detection results.

Fig. 9 goes here

As expected, we found that the synthetic core metrics were generally more normally distributed than the real core metrics metrics (Fig. 9). Synth1 (Density/Simplicity) and Synth2 (Late-Successional) exhibited skewness and kurtosis values closer to a normal distribution across most climate strata (Table S2). However, Synth3 (Post-Disturbance Recovery) retained a consistent negative skew (approx. -1.2 to -1.8) and high kurtosis (> 5.9), indicating a non-normal distribution (Table S2). Synth2 also showed some non-normality in the hot-dry-low Stratum 5 (Skew = 1.1, Kurtosis = 5.48; Table S2). Despite the general reduction in outlier-driven skewness via factor analysis, the endpoint values derived from our outlier approach still varied considerably across climate strata for all three synthetic metrics. For example, the upper endpoint for Synth2 ranged from a high of 3.62 in Stratum 1 to a low of 1.09 in Stratum 5 (Table S2). Similarly, the lower endpoint for Synth1 ranged from -3.45 in Stratum 3 to -2.29 in Stratum 4 (Table S2).

These results highlighted the efficacy and dual function of our chosen normalization strategy. While the issue of extreme, influential outliers was less pronounced with synthetic metrics, the

methodology remained useful for systematically capturing the biophysical context. The variation in endpoints suggested that the typical range for each ecological dimension was different depending on the local climate. The outlier-detection method therefore served as a robust and reproducible technique for identifying these stratum-specific endpoint ranges. Summary statistics of the synthetic core metrics and their endpoint values selected through the outlier-detection approach are presented in Table S2. Boxplots with quantile marks and the region within the endpoint values for the synthetic core metrics are shown in Figure 9.

3.3 Weight optimization

We implemented a data-driven optimization routine to derive weights that would equalize the influence of each metric on the final composite indicator. This routine aimed at avoiding the bias of “naive” or inherent weights, the subjectivity of “expert” weights, and the potential for undetected statistical artifacts. Our initial “naive” analysis of real core metrics, which did not attempt to equilibrate weights, revealed a substantial imbalance in the contribution of each real core metric, as measured by the proportion of variance explained in the composite indicator (Table 2). For instance, in Climate Stratum 4, the highly skewed eSE metric initially explained 47.1% of the composite indicator variance, while the more normally distributed SDI explained only 16.5%. This demonstrated that without intervention, the composite score would be disproportionately sensitive to changes in eSE. The application of our optimization algorithm successfully corrected this imbalance.

Table 2 goes here

Our optimization procedure systematically adjusted the weights, reducing the weight for real core metrics with high initial influence and increasing it for those with low influence, until a balanced solution was achieved (Table 2). The result was a near-perfect equalization of influence in every climate stratum, with each of the three real core metrics contributing approximately 33.3% of the variance to the final, optimized composite indicator. For example, in Stratum 4, the algorithm reduced the weight of eSE to 0.26 while increasing the weight of SDI to 0.42 to achieve this equilibrium.

A deeper analysis revealed that the initial imbalance resulting from the “naive” analysis was not primarily driven by inter-metric correlations (Becker et al., 2017, Suraci et al., 2023), which were generally low to moderate, but rather by the inherent statistical distribution of the metrics themselves (Table S1). We found a consistent relationship where metrics with highly skewed, non-normal distributions had a much larger initial influence on the composite. The eSE, which exhibited extreme positive skewness (e.g., > 3.3) and kurtosis (e.g., > 14.8) across all strata, consistently exerted the strongest initial influence in most cases. Conversely, SDI, which was the most normally distributed, often had the weakest initial influence. This suggests that the presence of extreme values and long tails in a metric’s distribution can cause it to statistically dominate a composite indicator if left unsupervised.

In the case of the synthetic core metrics, their initial (suboptimal) influence on the composite indicator was already well-balanced (Table 3). For example, in Climate Stratum 1, the initial variance explained by the three core synthetic metrics was 33.2%, 32.5%, and 34.3%, respectively, which was very close to the ideal 33.3% target of equalized influence. While some strata exhibited a moderate initial imbalance, the deviation was substantially smaller than that observed with the real core metrics. This result was an expected but desirable outcome of using principal factors as input metrics: their statistical construction promotes orthogonality and symmetric distributions, which in turn prevents single dimension from dominating the composite indicator. Although the initial composite was already well-balanced for the synthetic core metrics, we still applied the optimization algorithm as a final "fine-tuning" step to achieve a near-perfect influence equalization. After this final calibration, the influence of each synthetic core metric on the composite was equalized to approximately 33.3% across all strata (Table 3).

Table 3 goes here

3.4 Metric aggregation for the forest resilience composite indicator

The distributional properties of the final indicators, both across the landscape and within climate strata, reveal that the methodological choices made during their construction were not trivial, but rather had significant impacts on the final assessment of the forest resilience scores. The following subsections describe the differences in the outcomes given the overall pathway (Theoretical versus climate-stratified RCM and SCM), aggregation method (compensatory versus non-compensatory) and the information retention by type of metrics (real core versus synthetic core).

3.4.1 Composite indicator derivation

At the full landscape scale, we compared the Theoretical pathway (TPOR framework: no climate stratification, no optimized weighting, compensatory aggregation) to the two optimized pathways. The Theoretical pathway produced a composite indicator with a highly compressed distribution. Its total range of values (0.55 out of a maximum of 1.00) was only 55% of the RCM's range (1.00) and 58% of the SCM's range (0.95), and its interquartile range (IQR) of 0.09 showed that the central 50% of its values were packed into a narrower band than for the RCM (IQR = 0.14) or SCM (IQR = 0.13) pathways (Fig. 10). This compression was a direct consequence of the Theoretical pathway's landscape-wide min-max normalization, which flattened diverse ecological conditions into a narrow, centralized scale, masking the true extent of variability. While the resulting landscape-wide distribution was deceptively symmetric (Skewness = 0.07), this was likely an artifact of averaging many metrics, which obscured detail instead of revealing true central tendency. In contrast, the RCM and SCM pathways produced composites with much greater dispersion. This dispersion trend between the Theoretical pathway and the RCM and SCM pathways remained consistent across the five climate strata (Fig. 10). For instance, the RCM and SCM pathways revealed that the warmest and driest strata (4 and 5) exhibited the greatest internal variability in resilience scores (e.g., RCM IQR of 0.17 in Stratum 5 vs. 0.12 in Stratum 3), an important nuance missed by the Theoretical pathway

whose IQR remained consistently low (0.07-0.09) across all strata. Summary statistics of the Theoretical, RCM, and SCM composite indicators by climate strata and across the landscape are presented in Table S3.

Fig. 10 goes here

The comparison of the RCM and SCM pathways within and among climate strata revealed important differences (Fig. 10, Table S3). First, the median score and the max values for the RCM indicator were consistently higher than for the SCM indicator. Second, the SCM pathway consistently yielded a more symmetric distribution compared to the RCM pathway. For instance, in Stratum 1, the SCM skewness was -0.02 (nearly zero), while the RCM skewness was a more pronounced -0.53 and appeared to be driven by the higher max values. This pattern held constant across most strata and was a direct result of the SCM's statistically well-distributed synthetic inputs, making it an arguably more elegant approach. The RCM pathway inherited a faint signature of its sometimes-skewed real-metric inputs, which may be a desirable trait for managers who prefer indicators tied to directly measurable, tangible variables.

The analysis of the median scores for the RCM pathway indicated that four of the five climate strata (Strata 1, 2, 3, and 5) were consistently performing slightly above the midpoint of the score's range (0 to 1), achieving 55-56% of their respective forest resilience scores (Fig. 10, Table S3). Stratum 4 (one of the hottest and driest) stood out as a somewhat notable exception, with a lower median score of 0.50, indicating that its overall condition was less favorable compared to the rest of the landscape. The SCM pathway offered a slightly different, but equally insightful, narrative (Fig. 10, Table S3). Its results showed a significant consistency across the entire landscape, with the median scores of all five strata hovering very tightly around the midpoint of the score's range, between 0.49 and 0.51. This suggested that when viewed through the lens of the synthetic factors, the varied climatic zones were all performing at a nearly identical level, that is, approximately 50% of their intrinsic potential. The subtle difference between the core metric pathways, with the RCM identifying Stratum 4 as a lower-performing outlier and the SCM depicting broad-scale uniformity in relative performance, was a direct result of their different core metrics (real vs. synthetic) and highlighted how even rigorous, well-constructed indicators can lead to different nuances in interpretation.

3.4.2 Compensatory and non-compensatory aggregation

We compared the RCM and SCM pathways using both a compensatory (weighted arithmetic mean) and a non-compensatory (weighted geometric mean) approach. As outlined in the literature, a compensatory approach allows high performance in one metric to offset low performance in another, while a non-compensatory method heavily penalizes scores with one or more low metric values, and rewards balanced profiles. It is important to note that the non-compensatory approach was conducted on the original "naive" normalized metric values (no optimized weighting), as applying the influence-balancing weight optimization would defy the purpose of the non-compensatory aggregation by artificially masking the very imbalances it is designed to penalize. Thus, the comparison of compensatory and non-compensatory

aggregations serves to reveal the impact of one or more unfavorable metric values that would otherwise be masked in a compensatory approach.

The effect of applying a non-compensatory aggregation to the RCM pathway was not merely a shift, but a significant collapse of the indicator's values, exposing the severe imbalance among the underlying real core metrics (i.e., normalized metrics with disparate co-located values; Fig. 11). The median composite score in Climate Stratum 1 dropped from 0.565 in the compensatory model to a near-zero 0.053 in the non-compensatory model (Table S4). This indicated that the average location, while appearing satisfactory under a compensatory lens, was in fact deeply unbalanced, with high performance in one metric being completely undermined by critically low performance in another. This pattern held constant across all strata (Fig. 11). Furthermore, the shape of the distribution was radically transformed. The modest negative skew of the compensatory indicator (-0.65 in Stratum 1) was inverted into an extreme positive skew (1.42), coupled with very high kurtosis (5.50) (Table S4). This was the signature of a non-compensatory function applied to imbalanced data: the vast majority of scores are crushed into a "floor" near zero, with only a very long tail of rare, exceptionally well-balanced locations achieving higher scores. The SCM pathway also revealed the penalizing effect of non-compensation, but the impact was significantly less severe, confirming the more inherently balanced nature of the synthetic inputs (Fig. 11). In Stratum 1, the median score dropped from 0.497 (compensatory) to 0.105 (non-compensatory) (Table S4). While this was a substantial reduction, the resulting median value was nearly double that of the RCM pathway's non-compensatory score. This demonstrated that while the synthetic profiles also exhibited imbalances that were masked by simple averaging, they were far less extreme than those of the real core metrics. Similarly, the SCM indicator’s distribution shifted from being nearly perfectly symmetric (skewness of -0.03) to being moderately positively skewed (0.87), but to a much lesser degree than the RCM indicator (Table S4). Stratum-wise and across-landscape summary statistics of the RCM and SCM composite indicators based on compensatory and non-compensatory aggregation are presented in Table S4.

Fig. 11 goes here

A direct comparison of the two non-compensatory indicators revealed two different portraits of the landscape's condition when balance is required. The RCM non-compensatory indicator described a landscape where balanced, high-performing conditions were exceptionally rare. Its median scores were consistently and dramatically low (e.g., as low as 0.004 in Stratum 3), and its extreme positive skew indicated that the overwhelming majority of the landscape was in a state of severe metric imbalance (Table S4). In contrast, the SCM non-compensatory indicator, with higher median scores (e.g., 0.105 in Stratum 1) and less extreme skewness (Table S4), portrayed a landscape where imbalance existed but was not as critically pervasive. This stark difference highlighted a critical interpretive choice: the RCM non-compensatory indicator suggests that achieving balanced resilience is a rare, outlier condition based on tangible metrics, while the SCM non-compensatory counterpart suggests that from a smoothed, statistical perspective, the landscape has a more moderate and uniform level of balance.

3.5 Composite indicator sensitivity and performance evaluation

3.5.1 Information Retention Index

A central challenge in creating a composite indicator is the inevitable loss of information when a large, complex pool of metrics is reduced to a smaller, more manageable set. To quantify this loss, we developed and applied a novel, spatially-explicit, Information Retention Index (IRI), which measures the percentage of variance-weighted information from the initial ten metrics that is preserved by the selected core metrics across space. A higher IRI indicates a more effective and representative selection process. This analysis revealed a clear and consistent difference in the statistical efficiency of the RCM and SCM pathways.

The SCM pathway consistently demonstrated superior performance in retaining metric information compared to the RCM pathway, both at the landscape scale and by climate strata (Fig. 12, Table S5). The median IRI for the SCM pathway across all strata was 40.1%, indicating that its three synthetic factors successfully captured over 40% of the variance-weighted information from the original ten metrics. In contrast, the RCM pathway had a median IRI of 36.6%. While still substantial, this suggested that the selection of just three tangible metrics came at a quantifiable cost of information relative to the SCM approach. This result was expected: factor analysis is explicitly designed to create components that explain the maximum possible variance, whereas the RCM method, by selecting individual metrics, cannot fully account for the information contained in the metrics that were discarded.

Fig. 12 goes here

The pattern of SCM superior performance was also expressed across all climate strata (Fig. 12, Table S5). In all five zones, the SCM pathway yielded a higher median IRI than the RCM pathway. This performance gap was particularly pronounced in the driest, most stressed environments; in Climate Stratum 5, the SCM pathway retained 41.1% of the information, while the RCM pathway captured only 31.5%. The consistent outperformance of the SCM pathway across diverse ecological settings underscored the robustness and statistical power of using factor analysis for metric reduction.

3.5.2 Sensitivity analysis

To assess the robustness of our findings, we conducted a comprehensive sensitivity analysis to quantify how three critical methodological criteria, namely (1) normalization endpoints, (2) metric weights, and (3) aggregation method, influenced the final composite scores from the RCM and SCM pathways. We found that the two pathways exhibited fundamentally different sensitivity profiles, highlighting where the most critical methodological leverage exists in each approach (Fig. 13, Table S6). For the RCM pathway, the choice of aggregation method was the most influential criterion driving the final composite score, yielding a mean sensitivity index of 0.286 (potential range of 0 to 1). The wide confidence interval for the aggregation index (0.126 – 0.434) further indicated that the magnitude of its influence was not only large but also highly

variable, reinforcing its status as the most critical and uncertain methodological criterion for this pathway (Fig. 13). Metric weights was the second most sensitive parameter (0.217), followed by the choice of normalization endpoints (0.114). The high sensitivity to aggregation confirmed our earlier finding: the RCM's inputs (SDI, eSE, Snag40) were significantly imbalanced. Accordingly, the decision to allow or not allow compensation (i.e., choosing between a weighted arithmetic or geometric mean) was the single most impactful criterion. This decision significantly changed the indicator's final scores. The moderate sensitivity to endpoints reflected the skewed nature of the real metrics (especially eSE): because the distributions had long tails, the decision of where to define the metric's effective range had a non-trivial impact on the results. The framework's relative lack of sensitivity to weights was logical in this context: since the effect of aggregation was dominating, adjustments to the weights had a comparatively smaller influence on the final outcome.

Fig. 13 goes here

The Synthetic SCM pathway was more sensitive to the choice of metric weights, which registered an exceptionally high mean sensitivity index of 0.682 (Fig. 13, Table S6). This parameter also exhibited the widest confidence interval (0.448 – 0.906), denoting a high degree of uncertainty in its effect. The aggregation method (0.215) and endpoint selection (a negligible 0.012) were significantly less influential. This seemingly counterintuitive result validated the unique nature of the SCM approach. The synthetic metrics were, by design, statistically balanced and orthogonal. Their "naive" state was one of equal influence on the composite indicator. The SCM pathway's extreme sensitivity to weights resulted because of this inherent balance. Any deviation from equal weighting was a significant disruption to this influence equilibrium, and thus had a very large impact on the final composite score. Conversely, the SCM pathway showed almost no sensitivity to endpoint selection most likely because the synthetic factors were symmetrically distributed, and because the extreme outliers that make endpoints an issue for the RCM pathway were absent. This pathway was also less sensitive to the aggregation method since its inputs were already balanced, meaning the penalty applied by the non-compensatory geometric mean was much less severe. Statistics summarizing the sampled endpoint and weight values for the sensitivity analysis are presented in Table S7.

3.6 Pillar aggregation for ecosystem resilience representation across the Sierra Nevada

While our analysis focused on a single-level aggregation for clarity, the quantitative framework we developed is inherently modular and ideally suited for constructing more complex, multi-level hierarchical composite indicators. The core methodological steps, namely core metric selection (RCM or SCM), climate-based stratification, robust normalization, and weight optimization, can be applied iteratively at each stage of a hierarchical structure. For instance, we had an initial pool of metrics that were aggregated into each of the 10 pillars (e.g., fire dynamics, forest resilience, biodiversity conservation, economic diversity etc). These dimensions can be treated as new inputs for a second level of aggregation into one or more broader dimensions, in our case to make inferences about overall socio-ecological resilience, by again applying the same rigorous normalization and weighting procedures. As an example of the multi-level applicability

of our proposed framework, we followed the RCM and SCM pathways, including stratified normalization with endpoint selection and aggregation with optimized weights, for the 10 pillars defined by the TPOR Framework (Table S8). We then aggregated the resulting pillar scores to obtain the final Socio-Ecological Resilience score (Fig. 14). This nested application provided a consistent, data-driven engine for each aggregation step, removing the subjectivity often present in hierarchical models that rely on expert-assigned metrics and weights at different levels.

Fig. 14 goes here

4. Discussion

The construction of composite indicators to measure complex phenomena like socio-ecological resilience comes with methodological challenges that can lead to subjective, irreproducible, or ecologically ambiguous outcomes. This study confronted these challenges directly by developing and testing a quantitative, transparent, and adaptable framework. Our results demonstrate that the specific choices made during the indicator construction process, from metric selection and normalization to weighting and aggregation, are not merely technical details but are fundamental drivers of the final assessment, profoundly shaping its meaning, robustness, and ultimate utility for management.

4.1 Theoretical framework and stratification

A core principle highlighted in the literature is that a composite indicator must be grounded in a strong theoretical framework to be meaningful (Booysen, 2002; Burgass et al., 2017; Greco et al., 2019; Nardo et al., 2008). Our findings provide validation for this principle. The successful identification of the same three ecological dimensions of the forest resilience pillar, namely Structure, Composition, and Disturbance, through two independent statistical methods (ICLUST for the RCM pathway and factor analysis for the SCM pathway) confirms that our core metrics contained a coherent underlying structure aligned with our conceptual TPOR framework. Furthermore, our results underscore the inadequacy of a "one-size-fits-all" approach under the model of biophysical context for intrinsic ecological productivity (Jeronimo et al., 2019). The climate-based stratification successfully partitioned the study area into five statistically distinct ecological regions, each with a unique profile of productivity and water stress. The stratification step proved significant, as the subsequent normalization revealed that the expected range for a given metric often varied significantly among these strata. This variation aligns well with our assumption that what constitutes "favorable" or "unfavorable" values to promote resilience as part of the core metric normalization process should be context-dependent to account for intrinsic ecological capacity.

4.2 Counteracting statistical artifacts

The analysis of the core metrics revealed significant skewness and the presence of extreme outliers, particularly for the RCM pathway. These statistical properties are oftentimes

undesirable during normalization as they can lead to statistical artifacts on the resulting composite indicator, such as tightly compressed values within a small band around the mean (Tarasewicz and Jönsson, 2021). The application of our stratified, outlier-aware normalization method was therefore crucial for creating a stable indicator that was not disproportionately influenced by extreme values. Similarly, our stratum-constrained mathematical optimization of weights proved effective in balancing the contribution of each core metric on the final composite indicator. Studies have suggested using mathematical optimization techniques to balance the influence of metrics on the composite indicators (Becker et al., 2017; Paruolo et al., 2012; Suraci et al., 2023). The ideal outcome of the optimization process is a set of (unequal) weights, one for each metric, that when used in the aggregation process, results in the composite indicator being almost equally correlated to all the metrics. Our approach applied these optimization-based solutions in both pathways (RCM and SCM), and it demonstrated that a "naive" equal-weighting scheme would have allowed skewed metrics to dominate the final score. The optimization algorithm corrected this imbalance by systematically adjusting weights to ensure each core metric contributed equally. Interestingly, this step was less critical for the SCM pathway, whose statistically balanced inputs were already in a state of near-equal influence. This highlights a key insight: the necessity of a given methodological step is contingent on the nature of the inputs, and a robust framework should be able to account for this.

4.3 The trade-off between interpretability and representativeness

A central finding of this study is the characterization of the trade-off between the RCM and SCM pathways. The RCM pathway offers the significant advantage of using tangible, directly measurable metrics (e.g., Stand Density Index) that are easily understood by managers and stakeholders. Composite indicators derived from measurable metrics can be directly used to define and prioritize management actions across a landscape (Suraci et al., 2023; Tarasewicz and Jönsson, 2021). However, our Information Retention Index (IRI) revealed that this direct interpretability and usability comes at a quantifiable cost: the RCM pathway retained less of the total information from the initial dataset than its synthetic counterpart. Conversely, the FA-based SCM pathway, by design, over-performed at statistical representation, consistently achieving a higher IRI across the landscape and within every climate stratum. Outputs from FA (e.g., scores) can be used directly as synthetic metrics or as (sub-)indicators (Nicoletti et al, 2000) that efficiently represent the statistical dimensions of the data (Fusco, 2015). However, the cost of this statistical efficiency is the use of abstract metrics that are one step removed from direct physical measurement. Consequently, composite indicators based on techniques such as FA may present a challenge in informing how best to invest management to maintain or improve conditions (Hermans et al., 2008; Saisana and Tarantola, 2002).

The IRI was not used to declare a single "best" pathway. Rather it provided a measure of strength of representation for each pathway, highlighting the trade-off between direct interpretability and statistical representativeness. For RCM, the IRI provided a quantitative and repeatable measure of the RCM cost of selecting one core metric to represent a set of metrics - a quantified loss of information. As such, it quantified the cost of the RCM pathway's primary

benefit: the use of a single, directly measurable metric for each cluster. Similarly for SCM, the IRI reflected its primary benefit: its superior statistical efficiency and information retention. Overall, the explicit trade-off between the RCM and SCM pathways was reflected in the final composite indicators, where the RCM pathway identified Stratum 4 as a low-performing outlier while the SCM pathway depicted a landscape of more uniform relative performance, illustrating how these methodological choices can lead to different nuances in interpretation.

4.4 Aggregation, sensitivity, and the meaning of an indicator

The choice of aggregation method is a profound statement about the assumed nature of the system being measured. Our comparison of compensatory and non-compensatory aggregation methods illustrated this. For the RCM pathway, switching to a non-compensatory geometric mean caused the indicator scores to collapse, revealing that the seemingly acceptable scores from the compensatory method were masking severe underlying imbalances among the core metrics. This effect was far less severe for the more inherently balanced SCM pathway. This finding has critical management implications, suggesting that if balanced conditions are a prerequisite for resilience, the true state of the system may be much more precarious than a simple averaging of metrics would suggest. Finally, our sensitivity analysis provided a "user's guide" to the robustness of each pathway. It confirmed that the RCM indicator is most sensitive to the choice of aggregation method, while the SCM indicator is generally more sensitive to the choice of weights given its already balanced initial state. This pinpoints the largest sources of uncertainty in each framework, allowing for a more honest and responsible application of these tools.

4.5 Broader implications

The pathways for composite indicators presented in this study directly address the growing and urgent international call for robust, multi-dimensional, and spatially explicit assessments of forest resilience. The methodological challenges of constructing such assessments are no longer abstract academic concerns; they are now central to the implementation of landmark environmental policies and frameworks. Our work provides a feasible, generalized, and data-driven system that meets the specific needs articulated by these efforts, particularly regarding the demand for multi-dimensional indicators, the necessity of methodological simplification for practical application, and the requirement for advanced statistics to ensure transparency and rigor.

There is a clear global consensus that assessing and monitoring ecosystem resilience is fundamental to climate change adaptation. The IPCC Synthesis Report (IPCC, 2023) emphasizes with high confidence that maintaining the resilience of biodiversity and ecosystem services depends on effective and equitable conservation, and explicitly identifies monitoring as a key component of adaptation-related responses. For forests specifically, this implies a need to move beyond single-metric assessments (e.g., carbon storage) toward a more holistic, multi-dimensional understanding of ecosystem health and function. This need is made operational in several key policy initiatives. For instance, the European Union's Forest Resilience Monitoring

Framework explicitly calls for a system of indicators to track the multiple dimensions of forest resilience, including productivity, health, biodiversity, and protection against hazards like fire (Resco De Dios and Boer, 2025). Similarly, the Kunming-Montreal Global Biodiversity Framework (GBF) relies on a comprehensive monitoring system to track progress toward its 2030 targets, including Target 2, which aims to restore 30% of degraded ecosystems, thereby enhancing ecosystem resilience (Burgess et al., 2024). In the United States, legislation such as the pending Fix Our Forests Act mandates the identification of high-risk landscapes and the prioritization of treatments to increase resilience, a task that inherently requires a spatially explicit, multi-faceted assessment of ecological condition and risk of degradation or loss.

Our theoretical framework and composite indicator pathways directly answer this call. By grounding our assessment in the Ten Pillars of Resilience (TPOR) and offering complementary pathways for composite indicator derivation for pillars and ecosystems, we provide the multi-dimensional structure required by these initiatives. The final output is not a single, abstract number but a high-resolution map that allows managers to visualize and prioritize conservation and restoration needs and opportunities across a heterogeneous landscape, directly enabling the kind of strategic planning envisioned by these global and national efforts. Furthermore, the comprehensive breadth of pillars in the TPOR framework could enable it to serve a translational role across initiatives, serving as a common language for evaluating change and progress across multiple initiatives with varied individual metrics but shared pillars.

A primary challenge in large-scale monitoring is the tension between scientific completeness and practical feasibility. While a vast number of metrics can characterize an ecosystem, data availability is often inconsistent, and interpretation can become overwhelmingly complex for decision-makers. This is recognized in the Kunming-Montreal GBF, which proposes a limited number of "headline indicators" for high-level tracking and communication, supported by a broader suite of component and complementary indicators (Burgess et al., 2024). This GBF framework acknowledges the need for simplified, yet powerful, metrics that can be consistently applied. The Real Core Metrics (RCM) pathway developed in our study is a direct, quantitative solution to this challenge, and likely a more robust approach to selecting a limited set of indicators on which to base accomplishment, accountability, and policy. This pathway provides a scientifically defensible method for selecting a few representative "headline indicators" that global frameworks require, ensuring that simplification does not come at the cost of statistical representativeness. Furthermore, our novel Information Retention Index (IRI) quantifies the information cost of this simplification, providing a transparent measure of the trade-off between interpretation and statistical power, a critical step in building trust and credibility in the assessment process.

A recurring criticism of composite indicators is their susceptibility to methodological biases, particularly from subjective weighting schemes and normalization techniques that can distort results and mask underlying conditions. The "naive" equal-weighting of metrics, for instance, can allow statistically skewed or correlated variables to unintentionally dominate the final indicator score. Global frameworks like the GBF and the EU's monitoring system implicitly require that their indicators be robust, repeatable, and transparent to be credible for tracking

progress and ensuring accountability (Burgess et al., 2024; Resco De Dios and Boer, 2025). Our composite indicator pathway were explicitly designed to overcome these limitations with a suite of advanced statistical solutions:

Climate-Based Stratification: By first partitioning the landscape into distinct biophysical regions, we ensure that all subsequent analyses, particularly metric normalization, are ecologically context-dependent. This aligns with the IPCC's emphasis on regional and ecosystem-specific adaptation (IPCC, 2023) and avoids the statistical artifacts of a "one-size-fits-all" approach.

Data-Driven Weight Optimization: Instead of relying on subjective or equal weighting, our use of a stratum-constrained mathematical optimization algorithm systematically adjusts weights to ensure a balanced contribution from each core metric. This fully quantitative and reproducible process directly addresses the critique of arbitrary weighting and ensures the final composite is not unintentionally biased.

The Synthetic Core Metrics (SCM) Pathway: For applications where statistical rigor is crucial, our factor analysis-based SCM pathway offers a powerful alternative. By creating statistically independent, synthetic metrics, it reduces multicollinearity and maximizes the representation of the data variance, resulting in an exceptionally robust and efficient indicator. Furthermore, it offers a quantitatively robust and sensitive measure of change that reflects the values of individual metrics and their relationships with one another.

By replacing subjective decisions with these data-driven procedures, our pathways provide a blueprint for constructing forest resilience indicators that are transparent, adaptable, and defensible. It demonstrates that the process of building an indicator is as important as the final result, aligning with the need for credible and reliable tools to guide the monumental task of managing forest resilience in an era of global change.

5. Conclusions

The pathways we developed to derive and evaluate composite indicators of forest resilience address three of the most commonly identified barriers in global conservation and monitoring programs: 1) effectively identifying metrics that are tangible and actionable to build consensus for core metrics across multiple entities (agencies, states, countries); 2) reliably determining status and tracking change across the diverse and sometimes divergent components of socio-ecological systems (e.g., water, carbon, biodiversity, economics); and 3) sufficiently meeting both of these needs to credibly attribute benefits to policy and finance investments. These pathways are not only reproducible and transparent but also highly flexible and transferable. They are agnostic to the number of input metrics or hierarchical levels or spatial scales, making them scalable to different ecosystems and applications. The combination of the two pathways (RCM and SCM) offers a robust representation of conditions that can be used to meet the needs of multiple applications (i.e., regional, national and global initiatives). The ability to validate indicator values with the Information Retention Index and the post-hoc sensitivity analyses further enhances the ability for composite indicators to be transparent. Ultimately, the

dual-pathway approach combined with information retention and sensitivity analyses provides a robust and adaptable system for building multi-level forest ecosystem indicators to inform the significant, large-scale, high stakes investments required to mitigate forest degradation and loss.

CRediT authorship contribution statement

Bryan Fuentes: Methodology, Software, Formal analysis, Investigation, Data curation, Writing - original draft, Writing - review and editing, Visualization.

Patricia Manley: Conceptualization, Methodology, Resources, Writing - original draft, Visualization, Supervision, Project administration, Funding acquisition.

Nicholas Povak: Conceptualization, Methodology, Software, Validation, Formal analysis, Resources, Data curation, Writing - review & editing, Supervision, Project administration, Funding acquisition.

Acknowledgements

We would like to thank the Sierra Nevada Conservancy, California Tahoe Conservancy, U.S. Forest Service, and Resilient Forestry for providing funding and support to conduct and publish this research.

References

Barnard, S., & Elliott, M. (2015). The 10-tenets of adaptive management and sustainability: An holistic framework for understanding and managing the socio-ecological system. Environmental Science & Policy, 51, 181–191. https://doi.org/10.1016/j.envsci.2015.04.008

Barry, A. M., Hagar, J. C., & Rivers, J. W. (2017). Long-term dynamics and characteristics of snags created for wildlife habitat. Forest Ecology and Management, 403, 145–151. https://doi.org/10.1016/j.foreco.2017.07.049

Bastiaansen, R., Doelman, A., Eppinga, M. B., & Rietkerk, M. (2020). The effect of climate change on the resilience of ecosystems with adaptive spatial pattern formation. Ecology Letters, 23(3), 414–429. https://doi.org/10.1111/ele.13449

Becker, W., Caperna, G., Sorbo, M. D., Norlen, H., Papadimitriou, E., & Saisana, M. (2022). COINr: An R package for developing composite indicators. Journal of Open Source Software, 7(78), 4567. https://doi.org/10.21105/joss.04567

Becker, W., Saisana, M., Paruolo, P., & Vandecasteele, I. (2017). Weights and importance in composite indicators: Closing the gap. Ecological Indicators, 80, 12–22. https://doi.org/10.1016/j.ecolind.2017.03.056

1384 Benini, L., Bandini, V., Marazza, D., & Contin, A. (2010). Assessment of land use changes
1385 through an indicator-based approach: A case study from the Lamone river basin in Northern
1386 Italy. Ecological Indicators, 10(1), 4–14. https://doi.org/10.1016/j.ecolind.2009.03.016
1387
1388 Bollettino, V., Alcayna, T., Dy, P., & Vinck, P. (2017). Introduction to Socio-Ecological
1389 Resilience. Oxford University Press. https://doi.org/10.1093/acrefore/9780199389407.013.261
1390
1391 Booysen, F. (2002). An Overview and Evaluation of Composite Indices of Development. Social
1392 Indicators Research, 59(2), 115–151. https://doi.org/10.1023/A:1016275505152
1393
1394 Brand, F. (2009). Critical natural capital revisited: Ecological resilience and sustainable
1395 development. Ecological Economics, 68(3), 605–612.
1396 https://doi.org/10.1016/j.ecolecon.2008.09.013
1397
1398 Briguglio, L., Cordina, G., Farrugia, N., & Vella, S. (2009). Economic Vulnerability and
1399 Resilience: Concepts and Measurements. Oxford Development Studies, 37(3), 229–247.
1400 https://doi.org/10.1080/13600810903089893
1401
1402 Brovkina, O., Cienciala, E., Zemek, F., Lukeš, P., Fabianek, T., & Russ, R. (2017). Composite
1403 indicator for monitoring of Norway spruce stand decline. European Journal of Remote Sensing,
1404 50(1), 550–563. https://doi.org/10.1080/22797254.2017.1372697
1405
1406 Brunet, O. (2000). Calculation of composite leading indicators: A comparison of two different
1407 methods. In G. Poser & D. Bloesch (Eds.), Economic Surveys and Data Analysis (pp. 123–133).
1408 OECD Publishing.
1409
1410 Burgass, M. J., Halpern, B. S., Nicholson, E., & Milner-Gulland, E. J. (2017). Navigating
1411 uncertainty in environmental composite indicators. Ecological Indicators, 75, 268–278.
1412 https://doi.org/10.1016/j.ecolind.2016.12.034
1413
1414 Burgess, N. D., Ali, N., Bedford, J., Bhola, N., Brooks, S., Cierna, A., Correa, R., Harris, M.,
1415 Hargey, A., Hughes, J., McDermott-Long, O., Miles, L., Ravilious, C., Rodrigues, A. R., van
1416 Soesbergen, A., Sihvonen, H., Seager, A., Swindell, L., Vukelic, M., et al. (2024). Global Metrics
1417 for Terrestrial Biodiversity. Annual Review of Environment and Resources, 49(Volume 49,
1418 2024), 673–709. https://doi.org/10.1146/annurev-environ-121522-045106
1419
1420 Campos, F., Gomes, C., Malheiros, C., & Lima, L. S. (2024). Hospitality Environmental
1421 Indicators Enhancing Tourism Destination Sustainable Management. Administrative Sciences,
1422 14(3). https://doi.org/10.3390/admsci14030042
1423
1424 Chamberlain, C. P., Cova, G. R., Kane, V. R., Cansler, C. A., Kane, J. T., Bartl-Geller, B. N.,
1425 van Wagtendonk, L., Jeronimo, S. M. A., Stine, P., & North, M. P. (2023). Sierra Nevada
1426 reference conditions: A dataset of contemporary reference sites and corresponding remote

1427 sensing-derived forest structure metrics for yellow pine and mixed-conifer forests. Data in brief,
1428 51, 109807. https://doi.org/10.1016/j.dib.2023.109807
1429
1430 Chung, E.-S., & Lee, K. S. (2009). Prioritization of water management for sustainability using
1431 hydrologic simulation model and multicriteria decision making techniques. Journal of
1432 Environmental Management, 90(3), 1502–1511. https://doi.org/10.1016/j.jenvman.2008.10.008
1433
1434 Churchill, D. J., Larson, A. J., Dahlgreen, M. C., Franklin, J. F., Hessburg, P. F., & Lutz, J. A.
1435 (2013). Restoring forest resilience: From reference spatial patterns to silvicultural prescriptions
1436 and monitoring. Forest Ecology and Management, 291, 442–457.
1437 https://doi.org/10.1016/j.foreco.2012.11.007
1438
1439 Clark, R., Reed, J., & Sunderland, T. (2018). Bridging funding gaps for climate and sustainable
1440 development: Pitfalls, progress and potential of private finance. Land Use Policy, 71, 335–346.
1441 https://doi.org/10.1016/j.landusepol.2017.12.013
1442
1443 Cumming, G. S. (2011). Spatial resilience: integrating landscape ecology, resilience, and
1444 sustainability. Landscape Ecology, 26(7), 899–909. https://doi.org/10.1007/s10980-011-9623-1
1445
1446 Curtis, R. O., & Marshall, D. D. (2000). Technical Note: Why Quadratic Mean Diameter?
1447 Western Journal of Applied Forestry, 15(3), 137–139. https://doi.org/10.1093/wjaf/15.3.137
1448
1449 Cutter, S. L., Ash, K. D., & Emrich, C. T. (2014). The geographies of community disaster
1450 resilience. Global Environmental Change, 29, 65–77.
1451 https://doi.org/10.1016/j.gloenvcha.2014.08.005
1452
1453 Czúcz, B., Keith, H., Maes, J., Driver, A., Jackson, B., Nicholson, E., Kiss, M., & Obst, C.
1454 (2021). Selection criteria for ecosystem condition indicators. Ecological Indicators, 133, 108376.
1455 https://doi.org/10.1016/j.ecolind.2021.108376
1456
1457 Dale, V. H., & Beyeler, S. C. (2001). Challenges in the development and use of ecological
1458 indicators. Ecological Indicators, 1(1), 3–10. https://doi.org/10.1016/S1470-160X(01)00003-6
1459
1460 de Castro-Pardo, M., Martínez, P. F., & Zabaleta, A. P. (2022). An initial assessment of water
1461 security in Europe using a DEA approach. Sustainable Technology and Entrepreneurship, 1(1),
1462 100002. https://doi.org/10.1016/j.stae.2022.100002
1463
1464 De Groot, R. S., Blignaut, J., Van Der Ploeg, S., Aronson, J., Elmqvist, T., & Farley, J. (2013).
1465 Benefits of Investing in Ecosystem Restoration. Conservation Biology, 27(6), 1286–1293.
1466 http://www.jstor.org/stable/24480258
1467
1468 de Jonge, V. N., Pinto, R., & Turner, R. K. (2012). Integrating ecological, economic and social
1469 aspects to generate useful management information under the EU Directives' 'ecosystem

approach'. Ocean & Coastal Management, 68, 169–188. https://doi.org/10.1016/j.ocecoaman.2012.05.017

de Juan, S., Hewitt, J., Subida, M. D., & Thrush, S. (2018). Translating Ecological Integrity terms into operational language to inform societies. Journal of Environmental Management, 228, 319–327. https://doi.org/10.1016/j.jenvman.2018.09.034

De Leo, G. A., & Levin, S. (1997). The Multifaceted Aspects of Ecosystem Integrity. Conservation Ecology, 1(1). http://www.jstor.org/stable/26271649

De Montis, A., Serra, V., Ganciu, A., & Ledda, A. (2020). Assessing Landscape Fragmentation: A Composite Indicator. Sustainability, 12(22). https://doi.org/10.3390/su12229632

Dobrowski, S. Z., Abatzoglou, J., Swanson, A. K., Greenberg, J. A., Mynsberge, A. R., Holden, Z. A., & Schwartz, M. K. (2013). The climate velocity of the contiguous United States during the 20th century. Global Change Biology, 19(1), 241–251. https://doi.org/10.1111/gcb.12026

Ebert, U., & Welsch, H. (2004). Meaningful environmental indices: a social choice approach. Journal of Environmental Economics and Management, 47(2), 270–283. https://doi.org/10.1016/j.jeem.2003.09.001

Elsen, P. R., Monahan, W. B., Dougherty, E. R., & Merenlender, A. M. (2020). Keeping pace with climate change in global terrestrial protected areas. Science Advances, 6(25), eaay0814. https://doi.org/10.1126/sciadv.aay0814

Falk, D. A., van Mantgem, P. J., Keeley, J. E., Gregg, R. M., Guiterman, C. H., Tepley, A. J., Young, D. J., & Marshall, L. A. (2022). Mechanisms of forest resilience. Forest Ecology and Management, 512, 120129. https://doi.org/10.1016/j.foreco.2022.120129

Felipe-Lucia, M. R., Soliveres, S., Penone, C., Manning, P., van der Plas, F., Boch, S., Prati, D., Ammer, C., Schall, P., Gossner, M. M., Bauhus, J., Buscot, F., Blaser, S., Blüthgen, N., de Frutos, A., Ehbrecht, M., Frank, K., Goldmann, K., Hänsel, F., et al. (2018). Multiple forest attributes underpin the supply of multiple ecosystem services. Nature Communications, 9(1), 4839. https://doi.org/10.1038/s41467-018-07082-4

Ferrier, S., Harwood, T. D., Ware, C., & Hoskins, A. J. (2020). A globally applicable indicator of the capacity of terrestrial ecosystems to retain biological diversity under climate change: The bioclimatic ecosystem resilience index. Ecological Indicators, 117, 106554. https://doi.org/10.1016/j.ecolind.2020.106554

Flensborg, L. C., Maureaud, A. A., Bravo, D. N., & Lindegren, M. (2023). An indicator-based approach for assessing marine ecosystem resilience. ICES Journal of Marine Science, 80(5), 1487–1499. https://doi.org/10.1093/icesjms/fsad077

1514 Flint, L. E., Flint, A. L., & Stern, M. A. (2021). The basin characterization model: A regional
1515 water balance software package. U. S. Geological Survey; Techniques and Methods, p. 85.
1516 https://doi.org/10.3133/tm6H1
1517
1518 Forzieri, G., Dakos, V., McDowell, N. G., Ramdane, A., & Cescatti, A. (2022). Emerging signals
1519 of declining forest resilience under climate change. Nature, 608(7923), 534–539.
1520 https://doi.org/10.1038/s41586-022-04959-9
1521
1522 Franco-Gaviria, F., Amador-Jiménez, M., Millner, N., Durden, C., & Urrego, D. H. (2022).
1523 Quantifying resilience of socio-ecological systems through dynamic Bayesian networks.
1524 Frontiers in Forests and Global Change, 5. https://doi.org/10.3389/ffgc.2022.889274
1525
1526 Freudenberg, M. (2003). Composite Indicators of Country Performance: A Critical Assessment
1527 (Working Paper No. 16). OECD Publishing.
1528 https://EconPapers.repec.org/RePEc:oec:stiaaa:2003/16-en
1529
1530 Fusco, E. (2015). Enhancing non-compensatory composite indicators: A directional proposal.
1531 European Journal of Operational Research, 242(2), 620–630.
1532 https://doi.org/10.1016/j.ejor.2014.10.017
1533
1534 Gan, X., Fernandez, I. C., Guo, J., Wilson, M., Zhao, Y., Zhou, B., & Wu, J. (2017). When to use
1535 what: Methods for weighting and aggregating sustainability indicators. Ecological Indicators, 81,
1536 491–502. https://doi.org/10.1016/j.ecolind.2017.05.068
1537
1538 Gibari, S. E., Gómez, T., & Ruiz, F. (2018). Evaluating university performance using reference
1539 point based composite indicators. Journal of Informetrics, 12(4), 1235–1250.
1540 https://doi.org/10.1016/j.joi.2018.10.003
1541
1542 Gómez-Limón, J. A., Arriaza, M., & Guerrero-Baena, M. D. (2020). Building a Composite
1543 Indicator to Measure Environmental Sustainability Using Alternative Weighting Methods.
1544 Sustainability, 12(11). https://doi.org/10.3390/su12114398
1545
1546 Gorman, T., Kindermann, G., Healy, K., & Morley, T. R. (2024). Variation in ecological
1547 scorecards and their potential for wider use. Environmental Monitoring and Assessment, 196(8),
1548 722. https://doi.org/10.1007/s10661-024-12845-2
1549
1550 Gonon, M., Svartzman, R., & Althouse, J. (2024). Bridging the Gap in Biodiversity Financing: A
1551 review of assessments of existing and needed financial flows for biodiversity, and some
1552 considerations regarding their limitations and potential ways forward. UCL Institute for
1553 Innovation and Public Purpose, Working Paper Series. https://www.ucl.ac.uk/bartlett/public-
1554 purpose/WP2024-14
1555

1556 Greco, S., Ishizaka, A., Tasiou, M., & Torrisi, G. (2019). On the Methodological Framework of
1557 Composite Indices: A Review of the Issues of Weighting, Aggregation, and Robustness. Social
1558 Indicators Research, 141(1), 61–94. https://doi.org/10.1007/s11205-017-1832-9
1559
1560 Group of Seven. (2025, March 14). Statement of the G7 Kananaskis Wildfire Charter [Press
1561 release]. Government of Canada. https://g7.canada.ca/en/news-and-media/news/kananaskis-
1562 wildfire-charter
1563
1564 Hermans, E., den Bossche, F. V., & Wets, G. (2008). Combining road safety information in a
1565 performance index. Accident Analysis & Prevention, 40(4), 1337–1344.
1566 https://doi.org/10.1016/j.aap.2008.02.004
1567
1568 Hessburg, P. F., Miller, C. L., Parks, S. A., Povak, N. A., Taylor, A. H., Higuera, P. E., Prichard,
1569 S. J., North, M. P., Collins, B. M., Hurteau, M. D., Larson, A. J., Allen, C. D., Stephens, S. L.,
1570 Rivera-Huerta, H., Stevens-Rumann, C. S., Daniels, L. D., Gedalof, Z., Gray, R. W., Kane, V.
1571 R., et al. (2019). Climate, Environment, and Disturbance History Govern Resilience of Western
1572 North American Forests. Frontiers in Ecology and Evolution, 7.
1573 https://doi.org/10.3389/fevo.2019.00239
1574
1575 Hiete, M., Merz, M., Comes, T., & Schultmann, F. (2012). Trapezoidal fuzzy DEMATEL method
1576 to analyze and correct for relations between variables in a composite indicator for disaster
1577 resilience. OR Spectrum, 34(4), 971–995. https://doi.org/10.1007/s00291-011-0269-9
1578
1579 Holling, C. S. (1973). Resilience and Stability of Ecological Systems. Annual Review of Ecology
1580 and Systematics, 4, 1–23. https://doi.org/10.1146/annurev.es.04.110173.000245
1581
1582 IPCC. (2023) Climate Change 2023: Synthesis Report (H. Lee & J. Romero, eds.; p. 115).
1583 IPCC. https://doi.org/10.59327/IPCC/AR6-9789291691647
1584
1585 Iliadis, L., Skopianos, S., Tachos, S., & Spartalis, S. (2010). A Fuzzy Inference System Using
1586 Gaussian Distribution Curves for Forest Fire Risk Estimation. In H. Papadopoulos, A. S.
1587 Andreou, & M. Bramer (Eds.), Artificial Intelligence Applications and Innovations (pp. 376–386).
1588 Springer Berlin Heidelberg.
1589
1590 Huang, S., Ramirez, C., McElhaney, M., & Evans, K. (2018). F3: Simulating spatiotemporal
1591 forest change from field inventory, remote sensing, growth modeling, and management actions.
1592 Forest Ecology and Management, 415, 26-37. https://doi.org/10.1016/j.foreco.2018.02.026
1593
1594 Jeronimo, S. M. A., Kane, V. R., Churchill, D. J., Lutz, J. A., North, M. P., Asner, G. P., &
1595 Franklin, J. F. (2019). Forest structure and pattern vary by climate and landform across active-
1596 fire landscapes in the montane Sierra Nevada. Forest Ecology and Management, 437, 70–86.
1597 https://doi.org/10.1016/j.foreco.2019.01.033
1598

1599 Keane, R. E., Loehman, R. A., Holsinger, L. M., Falk, D. A., Higuera, P., Hood, S. M., & Hessburg, P. F. (2018). Use of landscape simulation modeling to quantify resilience for ecological applications. Ecosphere, 9(9), e02414. https://doi.org/10.1002/ecs2.2414

Keene, M., & Pullin, A. S. (2011). Realizing an effectiveness revolution in environmental management. Journal of Environmental Management, 92(9), 2130–2135. https://doi.org/10.1016/j.jenvman.2011.03.035

Klausmeyer, K. R., Shaw, M. R., MacKenzie, J. B., & Cameron, D. R. (2011). Landscape-scale indicators of biodiversity's vulnerability to climate change. Ecosphere, 2(8), art88. https://doi.org/10.1890/ES11-00044.1

Koltunov, A., Ramirez, C. M., Ustin, S. L., Slaton, M., & Haunreiter, E. (2020). eDaRT: The Ecosystem Disturbance and Recovery Tracker system for monitoring landscape disturbances and their cumulative effects. Remote Sensing of Environment, 238, 111482. https://doi.org/10.1016/j.rse.2019.111482

Kotzee, I., & Reyers, B. (2016). Piloting a social-ecological index for measuring flood resilience: A composite index approach. Ecological Indicators, 60, 45–53. https://doi.org/10.1016/j.ecolind.2015.06.018

Kouikoglou, V. S., & Phillis, Y. A. (2011). Application of a fuzzy hierarchical model to the assessment of corporate social and environmental sustainability. Corporate Social Responsibility and Environmental Management, 18(4), 209–219. https://doi.org/10.1002/csr.241

Lawler, J. J., Rinnan, D. S., Michalak, J. L., Withey, J. C., Randels, C. R., & Possingham, H. P. (2020). Planning for climate change through additions to a national protected area network: implications for cost and configuration. Philosophical Transactions of the Royal Society B: Biological Sciences, 375(1794), 20190117. https://doi.org/10.1098/rstb.2019.0117

Li, T., Zhang, H., Yuan, C., Liu, Z., & Fan, C. (2012). A PCA-based method for construction of composite sustainability indicators. The International Journal of Life Cycle Assessment, 17(5), 593–603. https://doi.org/10.1007/s11367-012-0394-y

Liggs, R., Schlüter, M., & Schoon, M. L. (2015). An introduction to the resilience approach and principles to sustain ecosystem services in social–ecological systems. In R. Biggs, M. Schlüter, & M. L. Schoon (Eds.), Principles for Building Resilience: Sustaining Ecosystem Services in Social-Ecological Systems (pp. 1–31). Cambridge University Press.

Lin, J. (2020). Developing a composite indicator to prioritize tree planting and protection locations. Science of the Total Environment, 717, 137269. https://doi.org/10.1016/j.scitotenv.2020.137269
1641

1642 Lü, D., & Lü, Y. (2021). Spatiotemporal variability of water ecosystem services can be effectively
1643 quantified by a composite indicator approach. Ecological Indicators, 130, 108061.
1644 https://doi.org/10.1016/j.ecolind.2021.108061
1645
1646 Lung, T., Lavalle, C., Hiederer, R., Dosio, A., & Bouwer, L. M. (2013). A multi-hazard regional
1647 level impact assessment for Europe combining indicators of climatic and non-climatic change.
1648 Global Environmental Change, 23(2), 522–536. https://doi.org/10.1016/j.gloenvcha.2012.11.009
1649
1650 Lutz, J. A., van Wagtendonk, J. W., & Franklin, J. F. (2010). Climatic water deficit, tree species
1651 ranges, and climate change in Yosemite National Park. Journal of Biogeography, 37(5), 936–
1652 950. https://doi.org/10.1111/j.1365-2699.2009.02268.x
1653
1654 Maechler, M., Rousseeuw, P., Struyf, A., Hubert, M., & Hornik, K. (2025). cluster: Cluster
1655 Analysis Basics and Extensions. https://CRAN.R-project.org/package=cluster
1656
1657 Manley, P. N., Bistritz, L., Povak, N. A., & Day, M. A. (2025). Going slow to go fast: landscape
1658 designs to achieve multiple benefits. Frontiers in Environmental Science, 13.
1659 https://doi.org/10.3389/fenvs.2025.1560125
1660
1661 Manley, P. N., Long, J. W., & Scheller, R. M. (2024). Keeping up with the landscapes: promoting
1662 resilience in dynamic social-ecological systems. Ecology and Society, 29(1).
1663 https://doi.org/10.5751/ES-14563-290103
1664
1665 Manley, P. N., Povak, N. A., Wilson, K. N., Fairweather, M. L., Griffey, V., & Long, L. L. (2023).
1666 Blueprint for resilience: the Tahoe-Central Sierra Initiative. U.S. Department of Agriculture,
1667 Forest Service, Pacific Southwest Research Station. https://doi.org/10.2737/psw-gtr-277
1668
1669 Marín, A. I., Malak, D. A., Bastrup-Birk, A., Chirici, G., Barbati, A., & Kleeschulte, S. (2021).
1670 Mapping forest condition in Europe: Methodological developments in support to forest
1671 biodiversity assessments. Ecological Indicators, 128, 107839.
1672 https://doi.org/10.1016/j.ecolind.2021.107839
1673
1674 Mazziotta, M., & Pareto, A. (2016). On a Generalized Non-compensatory Composite Index for
1675 Measuring Socio-economic Phenomena. Social Indicators Research, 127(3), 983–1003.
1676 https://doi.org/10.1007/s11205-015-0998-2
1677
1678 McDonald, G. T., & Lane, M. B. (2004). Converging global indicators for sustainable forest
1679 management. Forest Policy and Economics, 6(1), 63–70. https://doi.org/10.1016/S1389-
1680 9341(02)00101-6
1681
1682 Molinos-Senante, M., Gómez, T., Garrido-Baserba, M., Caballero, R., & Sala-Garrido, R.
1683 (2014). Assessing the sustainability of small wastewater treatment systems: A composite
1684 indicator approach. Science of the Total Environment, 497-498, 607–617.
1685 https://doi.org/10.1016/j.scitotenv.2014.08.026

1686 Munda, G. (2005). Multiple Criteria Decision Analysis and Sustainable Development. In Multiple
1687 Criteria Decision Analysis: State of the Art Surveys (pp. 953–986). Springer New York.
1688 https://doi.org/10.1007/0-387-23081-5_23
1689
1690 Munda, G., & Nardo, M. (2009). Noncompensatory/nonlinear composite indicators for ranking
1691 countries: a defensible setting. Applied Economics, 41(12), 1513–1523.
1692 https://doi.org/10.1080/00036840601019364
1693
1694 Munda, G., & Saisana, M. (2011). Methodological Considerations on Regional Sustainability
1695 Assessment Based on Multicriteria and Sensitivity Analysis. Regional Studies, 45(2), 261–276.
1696 https://doi.org/10.1080/00343401003713316
1697
1698 Nardo, M., Saisana, M., Saltelli, A., Tarantola, S., Hoffmann, A., & Giovannini, E. (2008).
1699 Handbook on Constructing Composite Indicators: Methodology and User Guide (2 ed.). OECD
1700 publishing. www.oecd.org/publishing, http://213.253.134.43/oecd/pdfs/browseit/3008251E.PDF
1701
1702 Nelder, J. A., & Mead, R. (1965). A Simplex Method for Function Minimization. The Computer
1703 Journal, 7(4), 308–313. https://doi.org/10.1093/comjnl/7.4.308
1704
1705 Newton, A. C., & Cantarello, E. (2015). Restoration of forest resilience: An achievable goal?
1706 New Forests, 46(5), 645–668. https://doi.org/10.1007/s11056-015-9489-1
1707
1708 Nicoletti, G., Scarpetta, S., & Boylaud, O. (2000). Summary Indicators of Product Market
1709 Regulation with an Extension to Employment Protection Legislation (Working Paper No. 226).
1710 OECD Publishing. https://doi.org/10.1787/215182844604
1711
1712 Paruolo, P., Saisana, M., & Saltelli, A. (2012). Ratings and Rankings: Voodoo or Science?
1713 Journal of the Royal Statistical Society Series A: Statistics in Society, 176(3), 609–634.
1714 https://doi.org/10.1111/j.1467-985X.2012.01059.x
1715
1716 Payn, T. W., Downey, M., Han, H., Howell, C., Klinger, S., Matsuura, T., Robertson, G., &
1717 Sadiq, T. (2023). Montreal Process: Synthesis of indicator trends 1990 to 2020 and future
1718 outlooks (T. W. Payn, ed.; p. 44). Scion. https://montreal-process.org/documents/publications
1719
1720 Perino, A., Pereira, H. M., Felipe-Lucia, M., Kim, H., Kühl, H. S., Marselle, M. R., Meya, J. N.,
1721 Meyer, C., Navarro, L. M., van Klink, R., Albert, G., Barratt, C. D., Bruelheide, H., Cao, Y.,
1722 Chamoin, A., Darbi, M., Dornelas, M., Eisenhauer, N., Essl, F., et al. (2022). Biodiversity post-
1723 2020: Closing the gap between global targets and national-level implementation. Conservation
1724 Letters, 15(2), e12848. https://doi.org/10.1111/conl.12848
1725
1726 Pert, P. L., Butler, J. R. A., Bruce, C., & Metcalfe, D. (2012). A composite threat indicator
1727 approach to monitor vegetation condition in the Wet Tropics, Queensland, Australia. Ecological
1728 Indicators, 18, 191–199. https://doi.org/10.1016/j.ecolind.2011.11.018
1729

1730 Povak, N. A., & Manley, P. N. (2024). Evaluating climate change impacts on ecosystem
1731 resources through the lens of climate analogs. Frontiers in Forests and Global Change, 6.
1732 https://doi.org/10.3389/ffgc.2023.1286980
1733
1734 Povak, N. A., Manley, P. N., & Wilson, K. N. (2024). Quantitative methods for integrating climate
1735 adaptation strategies into spatial decision support models. Frontiers in Forests and Global
1736 Change, 7. https://doi.org/10.3389/ffgc.2024.1286937
1737
1738 Puyenbroeck, T. V., & Rogge, N. (2017). Geometric mean quantity index numbers with Benefit-
1739 of-the-Doubt weights. European Journal of Operational Research, 256(3), 1004–1014.
1740 https://doi.org/10.1016/j.ejor.2016.07.038
1741
1742 Reich, K. F., Kunz, M., Bitter, A. W., & Von Oheimb, G. (2022). Do different indices of forest
1743 structural heterogeneity yield consistent results? iForest - Biogeosciences and Forestry, 5, 424–
1744 432. https://doi.org/10.3832/ifor4096-015
1745
1746 Resco De Dios, V., & Boer, M. M. (2025). EU forest monitoring should combine up-to-date
1747 science with best practice. Nature Ecology & Evolution, 9(5), 743–744.
1748 https://doi.org/10.1038/s41559-025-02672-0
1749
1750 Revelle, W. (1979). Hierarchical Cluster Analysis And The Internal Structure Of Tests.
1751 Multivariate Behavioral Research, 14(1), 57–74. https://doi.org/10.1207/s15327906mbr1401_4
1752
1753 Reyer, C. P. O., Rammig, A., Brouwers, N., & Langerwisch, F. (2015). Forest resilience, tipping
1754 points and global change processes. Journal of Ecology, 103(1), 1–4.
1755 https://doi.org/10.1111/1365-2745.12342
1756
1757 Riedler, B., Pernkopf, L., Strasser, T., Lang, S., & Smith, G. (2015). A composite indicator for
1758 assessing habitat quality of riparian forests derived from Earth observation data. International
1759 Journal of Applied Earth Observation and Geoinformation, 37, 114–123.
1760 https://doi.org/10.1016/j.jag.2014.09.006
1761
1762 Rousseeuw, P. J. (1987). Silhouettes: A graphical aid to the interpretation and validation of
1763 cluster analysis. Journal of Computational and Applied Mathematics, 20, 53–65.
1764 https://doi.org/10.1016/0377-0427(87)90125-7
1765
1766 Saisana, M., & Saltelli, A. (2011). Rankings and Ratings: Instructions for Use. Hague Journal on
1767 the Rule of Law, 3(2), 247–268. https://doi.org/10.1017/S1876404511200058
1768
1769 Saisana, M., & Tarantola, S. (2002). State-of-the-art report on current methodologies and
1770 practices for composite indicator development. European Commission, Joint Research Centre,
1771 Institute for the Protection and the Security of the Citizen, Technological and Economic Risk
1772 Management Unit.
1773

1774 Saisana, M., Saltelli, A., & Tarantola, S. (2005). Uncertainty and Sensitivity Analysis Techniques
1775 as Tools for the Quality Assessment of Composite Indicators. Journal of the Royal Statistical
1776 Society Series A: Statistics in Society, 168(2), 307–323. https://doi.org/10.1111/j.1467-
1777 985X.2005.00350.x
1778
1779 Salvati, L., Tombolini, I., Perini, L., & Ferrara, A. (2013). Landscape changes and environmental
1780 quality: the evolution of land vulnerability and potential resilience to degradation in Italy.
1781 Regional Environmental Change, 13(6), 1223–1233. https://doi.org/10.1007/s10113-013-0437-3
1782
1783 Sawyer, J., Keeler-Wolf, T., & Evans, J. (2008). The manual of California vegetation (2 ed.).
1784 Springer.
1785
1786 Scheffer, M., & Carpenter, S. R. (2003). Catastrophic regime shifts in ecosystems: linking theory
1787 to observation. Trends in Ecology & Evolution, 18(12), 648–656.
1788 https://doi.org/10.1016/j.tree.2003.09.002
1789
1790 Sharifi, A., & Yamagata, Y. (2016). Urban Resilience Assessment: Multiple Dimensions, Criteria,
1791 and Indicators. In Y. Yamagata & H. Maruyama (Eds.), Urban Resilience: A Transformative
1792 Approach (pp. 259–276). Springer International Publishing. https://doi.org/10.1007/978-3-319-
1793 39812-9_13
1794
1795 Singh, R. K., Murty, H. R., Gupta, S. K., & Dikshit, A. K. (2007). Development of composite
1796 sustainability performance index for steel industry. Ecological Indicators, 7(3), 565–588.
1797 https://doi.org/10.1016/j.ecolind.2006.06.004
1798
1799 Sturtevant, B. R., Miranda, B. R., Wolter, P. T., James, P. M. A., Fortin, M.-J., & Townsend, P.
1800 A. (2014). Forest recovery patterns in response to divergent disturbance regimes in the Border
1801 Lakes region of Minnesota (USA) and Ontario (Canada). Forest Ecology and Management, 313,
1802 199–211. https://doi.org/10.1016/j.foreco.2013.10.039
1803
1804 Suraci, J. P., Farwell, L. S., Littlefield, C. E., Freeman, P. T., Zachmann, L. J., Landau, V. A.,
1805 Anderson, J. J., & Dickson, B. G. (2023). Achieving conservation targets by jointly addressing
1806 climate change and biodiversity loss. Ecosphere, 14(4). https://doi.org/10.1002/ecs2.4490
1807
1808 Talukder, B., W. Hipel, K., & vanLoon, W. (2017). Developing Composite Indicators for
1809 Agricultural Sustainability Assessment: Effect of Normalization and Aggregation Techniques.
1810 Resources, 6(4). https://doi.org/10.3390/resources6040066
1811
1812 Tarasewicz, N. A., & Jönsson, A. M. (2021). An ecosystem model based composite indicator,
1813 representing sustainability aspects for comparison of forest management strategies. Ecological
1814 Indicators, 133, 108456. https://doi.org/10.1016/j.ecolind.2021.108456
1815

1816 Tate, E. (2012). Social vulnerability indices: a comparative assessment using uncertainty and
1817 sensitivity analysis. Natural Hazards, 63(2), 325–347. https://doi.org/10.1007/s11069-012-0152-
1818 2
1819
1820 Thakur, D. A., & Mohanty, M. P. (2025). Utilizing Multi-criteria Decision-Making Techniques for
1821 Computing Composite Vulnerability over a Severely Flood-Prone Multi-hazard Catchment. In J.
1822 Das & S. Halder (Eds.), Progress in Multicriteria Decision Making Models: A New Paradigm to
1823 Monitor Hazards (pp. 291–309). Springer Nature Switzerland. https://doi.org/10.1007/978-3-
1824 031-89246-2_12
1825
1826 Thompson, B. S. (2023). Impact investing in biodiversity conservation with bonds: An analysis of
1827 financial and environmental risk. Business Strategy and the Environment, 32(1), 353–368.
1828 https://doi.org/10.1002/bse.3135
1829
1830 van Oudenhoven, A. P. E., Petz, K., Alkemade, R., Hein, L., & De Groot, R. S. (2012).
1831 Framework for systematic indicator selection to assess effects of land management on
1832 ecosystem services. Ecological Indicators, 21, 110–122.
1833 https://doi.org/10.1016/j.ecolind.2012.01.012
1834
1835 Waldron, A., Mooers, A. O., Miller, D. C., Nibbelink, N., Redding, D., Kuhn, T. S., Roberts, J. T.,
1836 & Gittleman, J. L. (2013). Targeting global conservation funding to limit immediate biodiversity
1837 declines. Proceedings of the National Academy of Sciences, 110(29), 12144–12148.
1838 https://doi.org/10.1073/pnas.1221370110
1839
1840 Wang, X., & Cumming, S. G. (2011). Measuring landscape configuration with normalized
1841 metrics. Landscape Ecology, 26(5), 723–736. https://doi.org/10.1007/s10980-011-9601-7
1842
1843 Yamada, S. B., Fisher, J. L., & Kosro, P. M. (2021). Relationship between ocean ecosystem
1844 indicators and year class strength of the invasive European green crab (Carcinus maenas).
1845 Progress in Oceanography, 196, 102618. https://doi.org/10.1016/j.pocean.2021.102618
1846
1847 Ye, Y., & Link, J. S. (2023). A composite fishing index to support the monitoring and sustainable
1848 management of world fisheries. Scientific Reports, 13(1), 10571.
1849 https://doi.org/10.1038/s41598-023-37048-6
1850
1851 Yu, D., Lu, N., & Fu, B. (2017). Establishment of a comprehensive indicator system for the
1852 assessment of biodiversity and ecosystem services. Landscape Ecology, 32(8), 1563–1579.
1853 https://doi.org/10.1007/s10980-017-0549-0
1854
1855 Zadeh, L. A. (1965). Fuzzy sets. Information and Control, 8(3), 338–353.
1856 https://doi.org/10.1016/S0019-9958(65)90241-X
1857
1858 Zani, S., Milioli, M. A., & Morlini, I. (2013). Fuzzy Composite Indicators: An Application for
1859 Measuring Customer Satisfaction. In N. Torelli, F. Pesarin, & A. Bar-Hen (Eds.), Advances in

Theoretical and Applied Statistics (pp. 243–253). Springer Berlin Heidelberg. https://doi.org/10.1007/978-3-642-35588-2_23

zu Ermgassen, S. O. S. E., & Löfqvist, S. (2024). Financing ecosystem restoration. Current Biology, 34(9), R412–R417. https://doi.org/10.1016/j.cub.2024.02.031

Figures and Captions

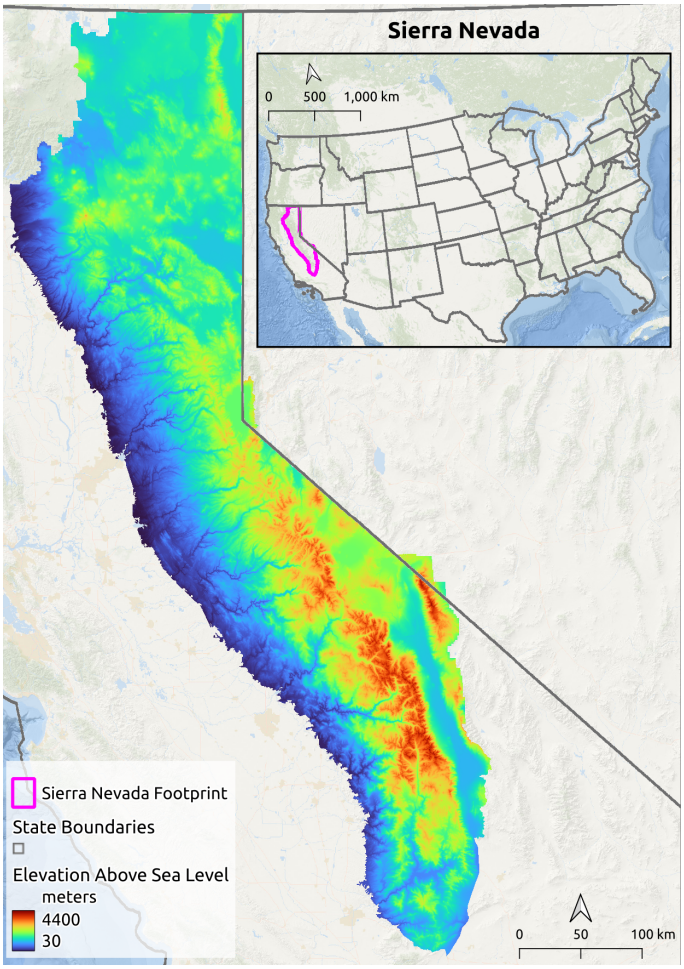

Figure 1: The Sierra Nevada, California, demonstration landscape.

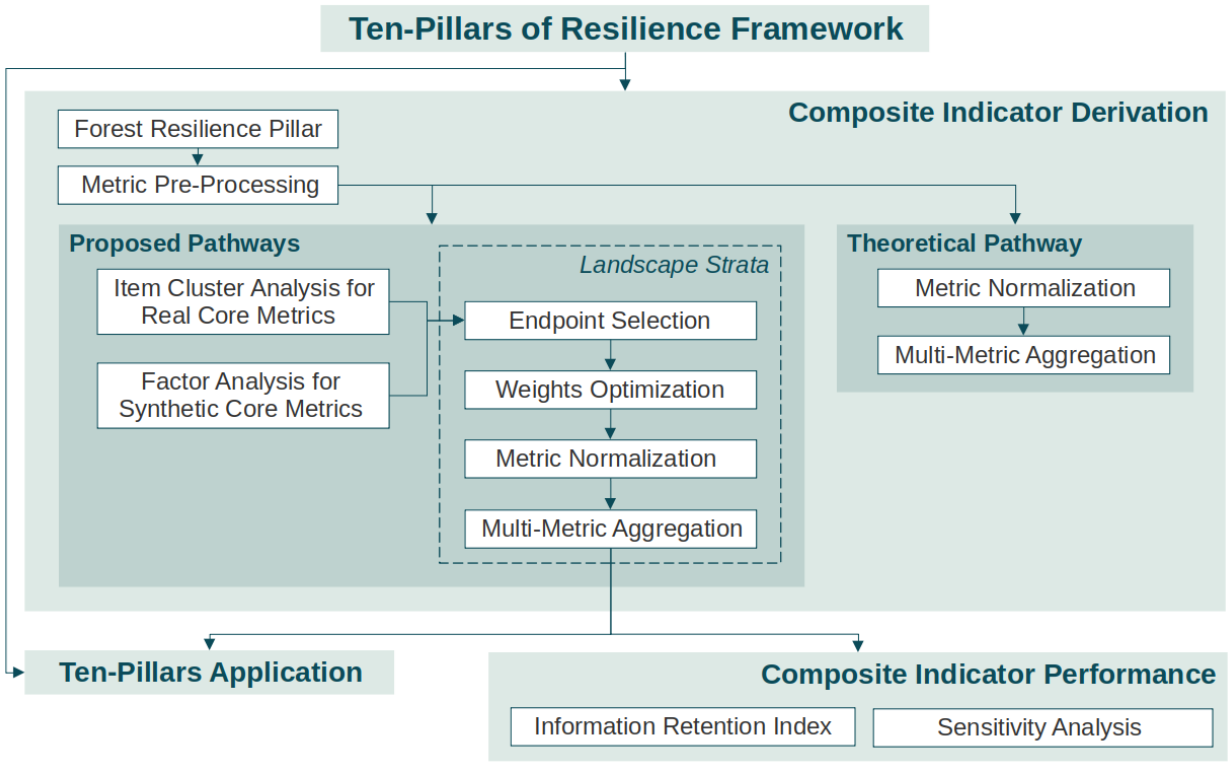

Figure 2: Schematic representation of the proposed workflow to build composite indicators of forest resilience based on two analytical pathways. The first pathway is based on hierarchical cluster analysis to select 'core' metrics from a large pool of initial metrics. The second pathway has the same objective but it employs factor analysis to build 'synthetic' core metrics. These two pathways include landscape stratification to constraint endpoint selection based on outlier detection, mathematical weight optimization, metric normalization based on fuzzy logic, and metric aggregation via compensatory or non-compensatory means. The composite indicator performance is assessed through a spatially-explicit information retention index and sensitivity analysis. A third (theoretical) pathway is presented for comparison purposes.

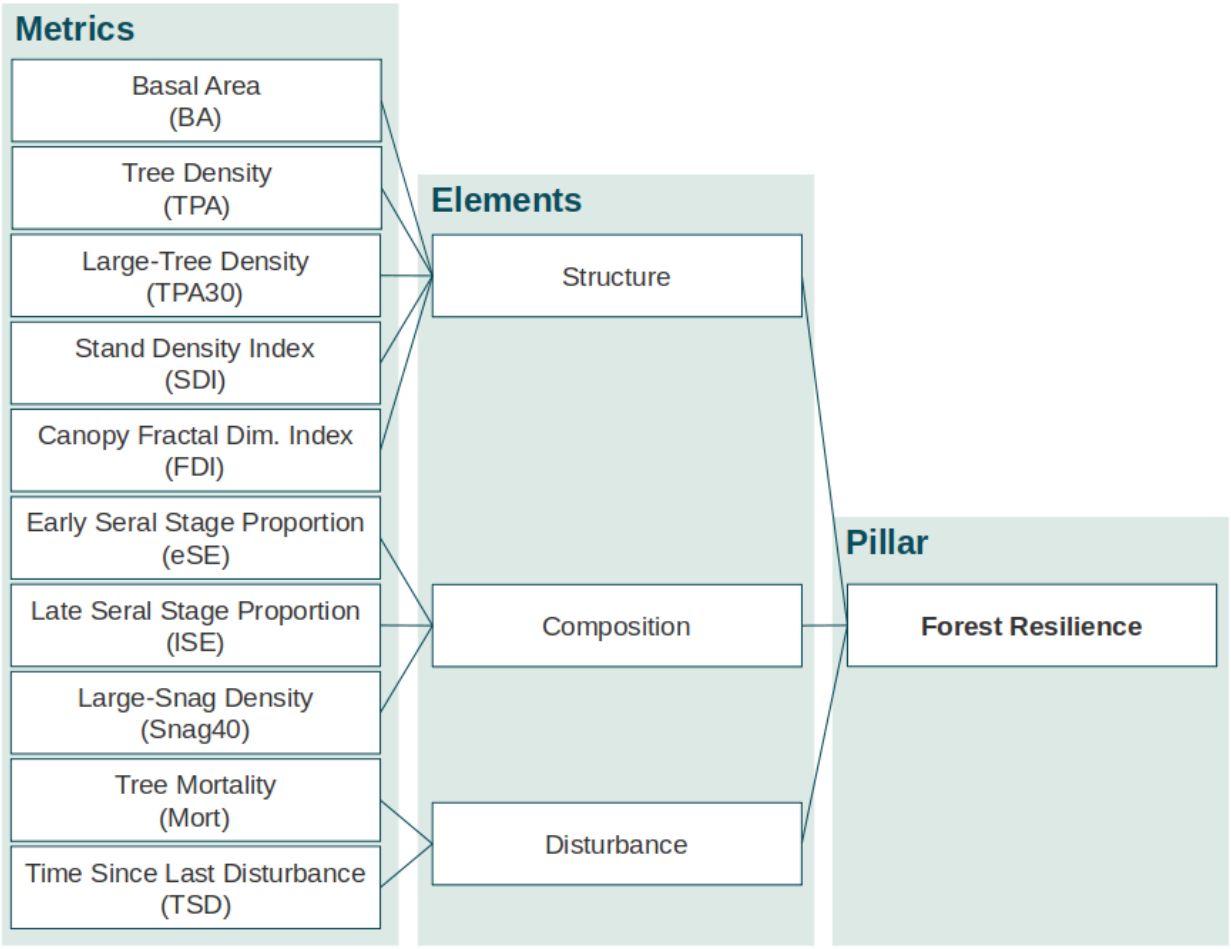

Figure 3: Ten metrics of forest resilience used to demonstrate composite indicator methodologies. They represent the three elements of the forest resilience pillar of the TPOR Framework, and illustrate the hierarchical structure of the pillar that served as the theoretical foundation for building the composite indicator.

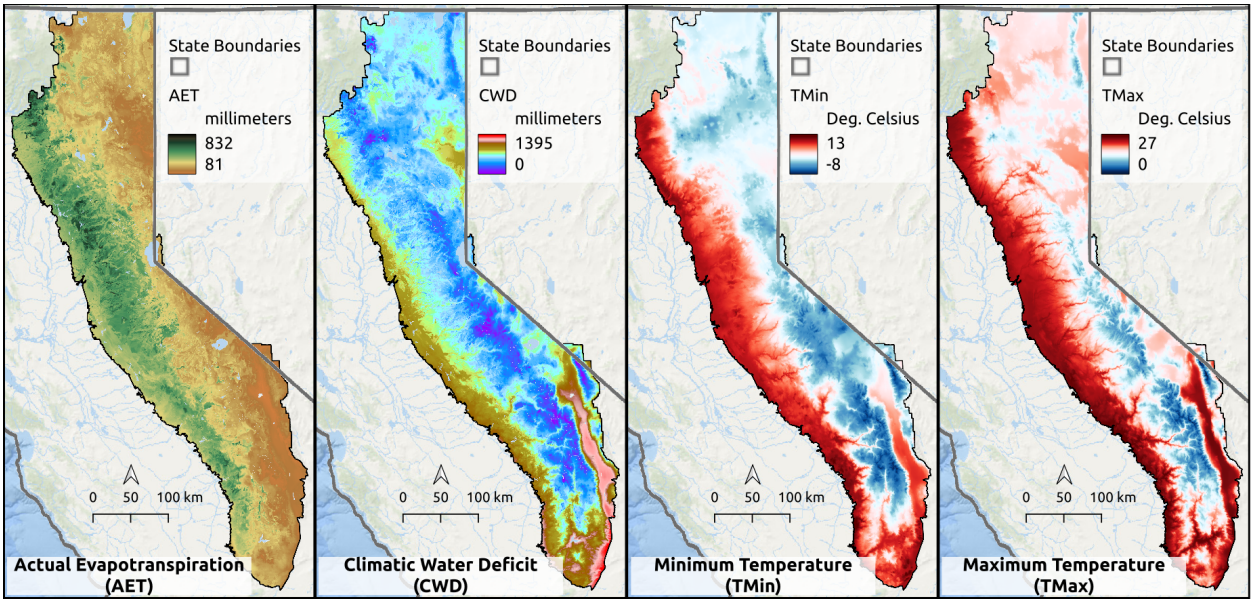

Figure 4: Maps of the four variables used in a cluster analysis to generate climate strata for the Sierra Nevada, California: a) actual evapotranspiration (AET in millimeters), b) climatic water deficit (CWD in millimeters), c) minimum annual temperature (TMin in centigrade), and d) maximum annual temperature (TMax in centigrade). Data values represent 30-year normals (1981-2010; Flint et al., 2021).

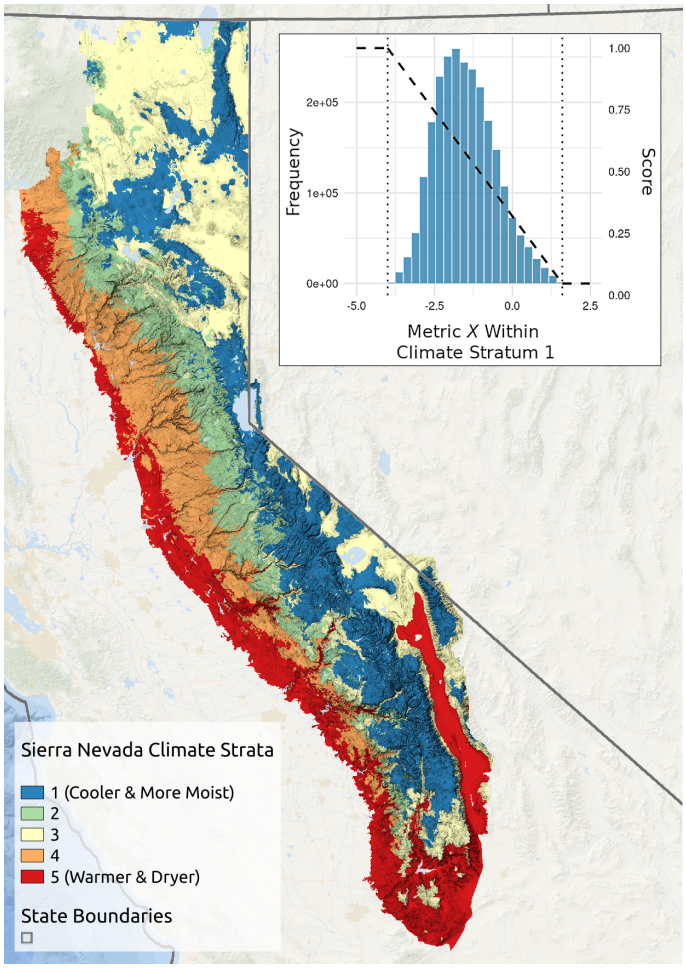

Figure 5: A schematic representation of the stratified normalization process for ten metrics of forest resilience based on fuzzy logic and endpoint values. The dotted, vertical bars in the inset histogram represent the lower (left) and upper (right) endpoint values for a given metric X within the climate stratum 1 (cooler and more moist). The z-shaped dotted line in the same inset represents the fuzzy logic membership function used for stratum-wise, endpoint-constrained metric normalization.

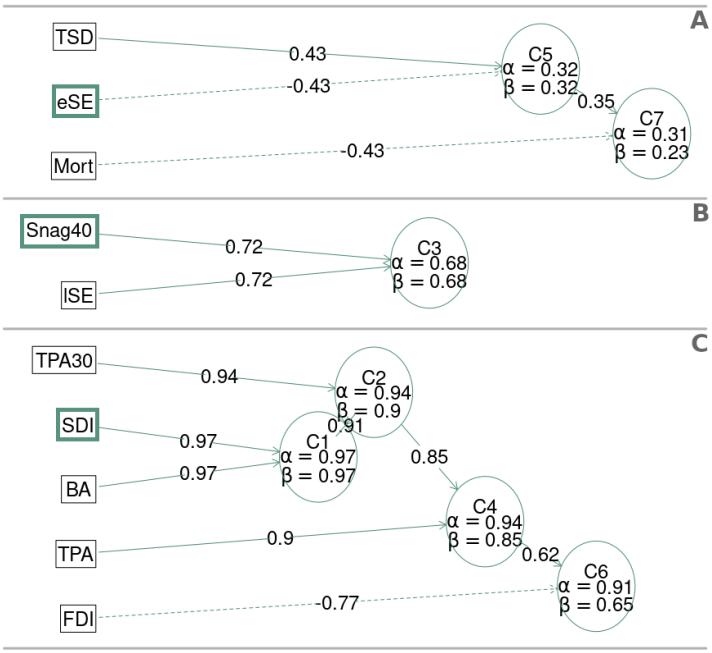

Figure 6: Results of the item cluster analysis (ICLUST) (Revelle, 1979) performed to select real core metrics (RCM) from the ten metrics of forest resilience across the Sierra Nevada, California. The subsets A, B, and C, represent the three metric clusters found through ICLUST (disturbance-centric, composition-centric, and structure-centric, respectively). The bold frames denote the forest resilience metrics selected as core metrics for each cluster.

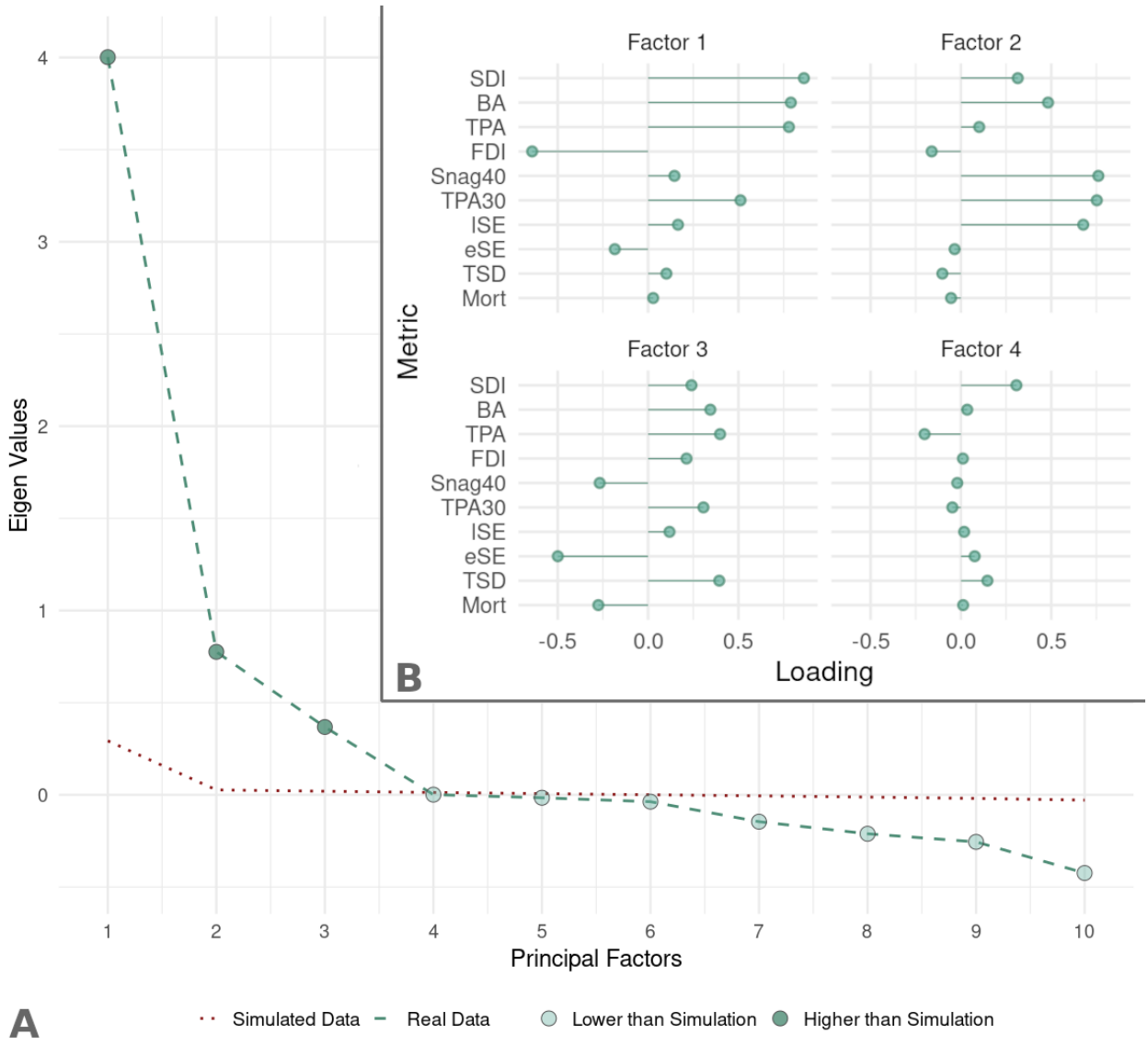

Figure 7: Factor analysis of ten metrics of forest resilience across the Sierra Nevada, California, including the random parallel simulation and factor loadings.

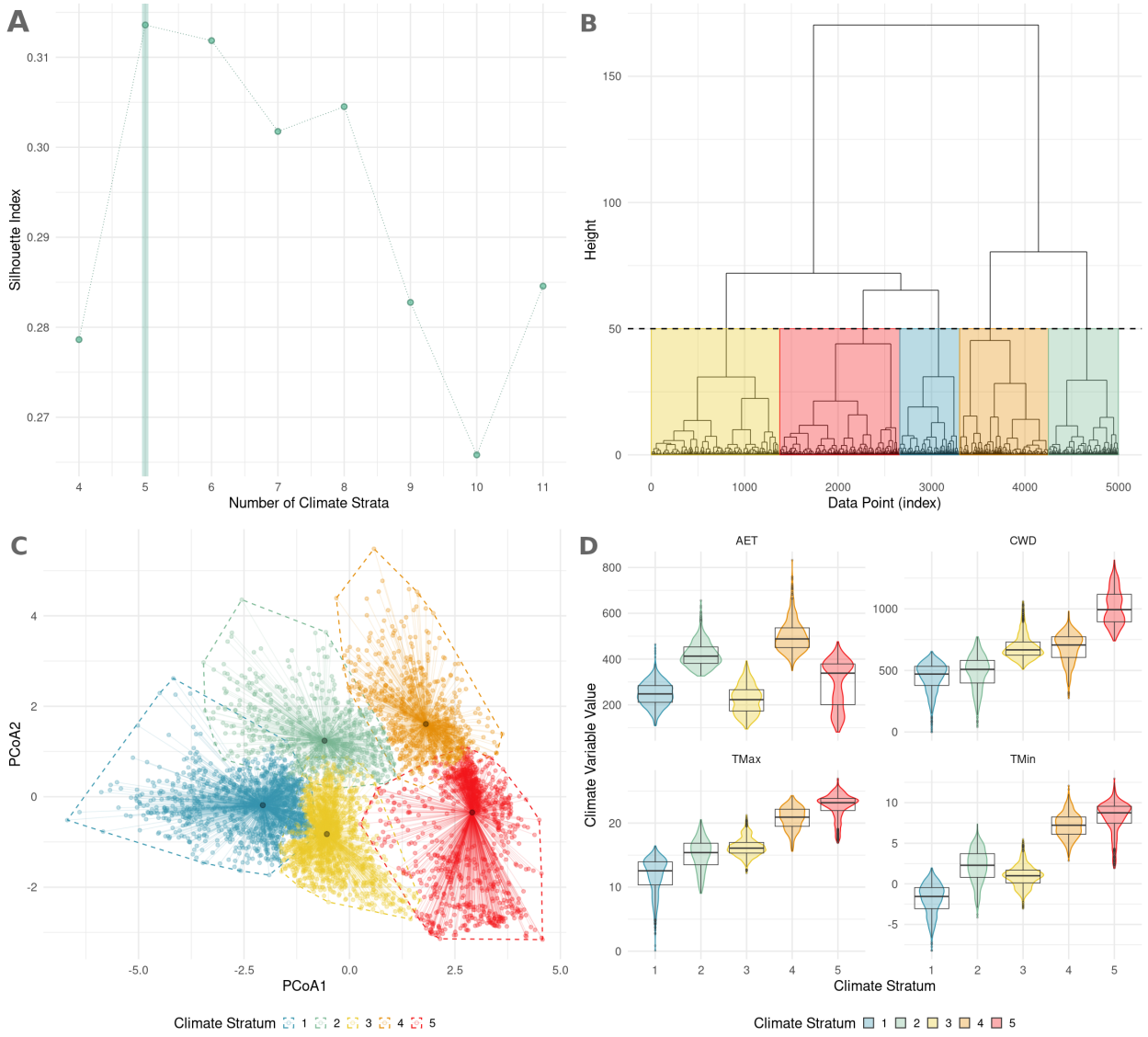

Figure 8: Silhouette index for a chain of hierarchical cluster analysis with different number of clusters (k, i.e., climate strata) (A), dendrogram partitioned at the clustering solution with the highest silhouette index value (k = 5) (B), Projection of the points sampled for cluster analysis onto the first two principal coordinate axes (C), and stratum-wise boxplots and violin plots of the input climate variables for cluster analysis (D).

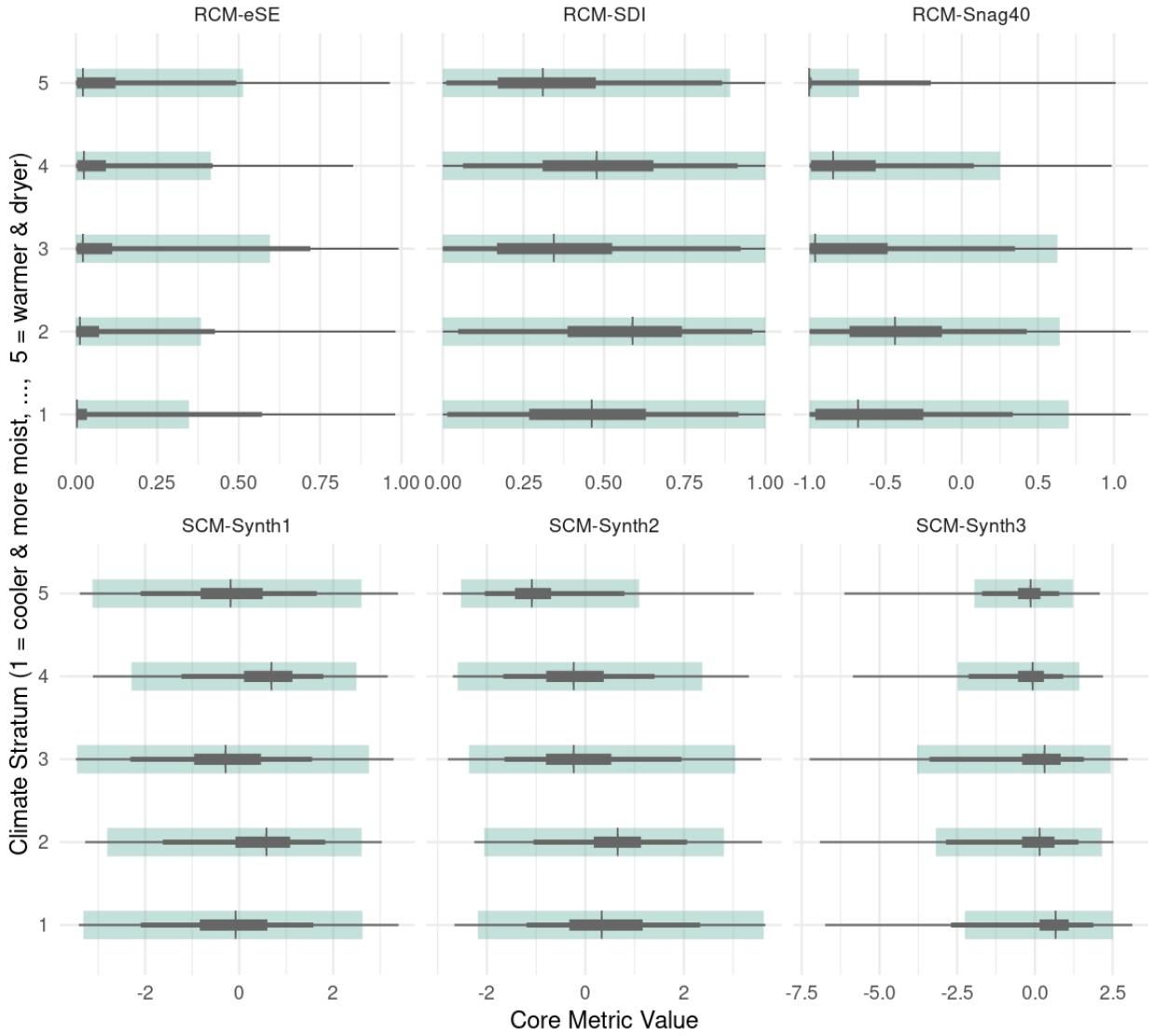

Figure 9: Boxplots showing the statistical distribution of the real core metrics (RCM) and synthetic core metrics SCM) representing forest resilience across the Sierra Nevada, California. The statistics are summarized for each climate stratum mapped across the landscape. The shaded region in each boxplot represents the range within the endpoint values selected through outlier detection.

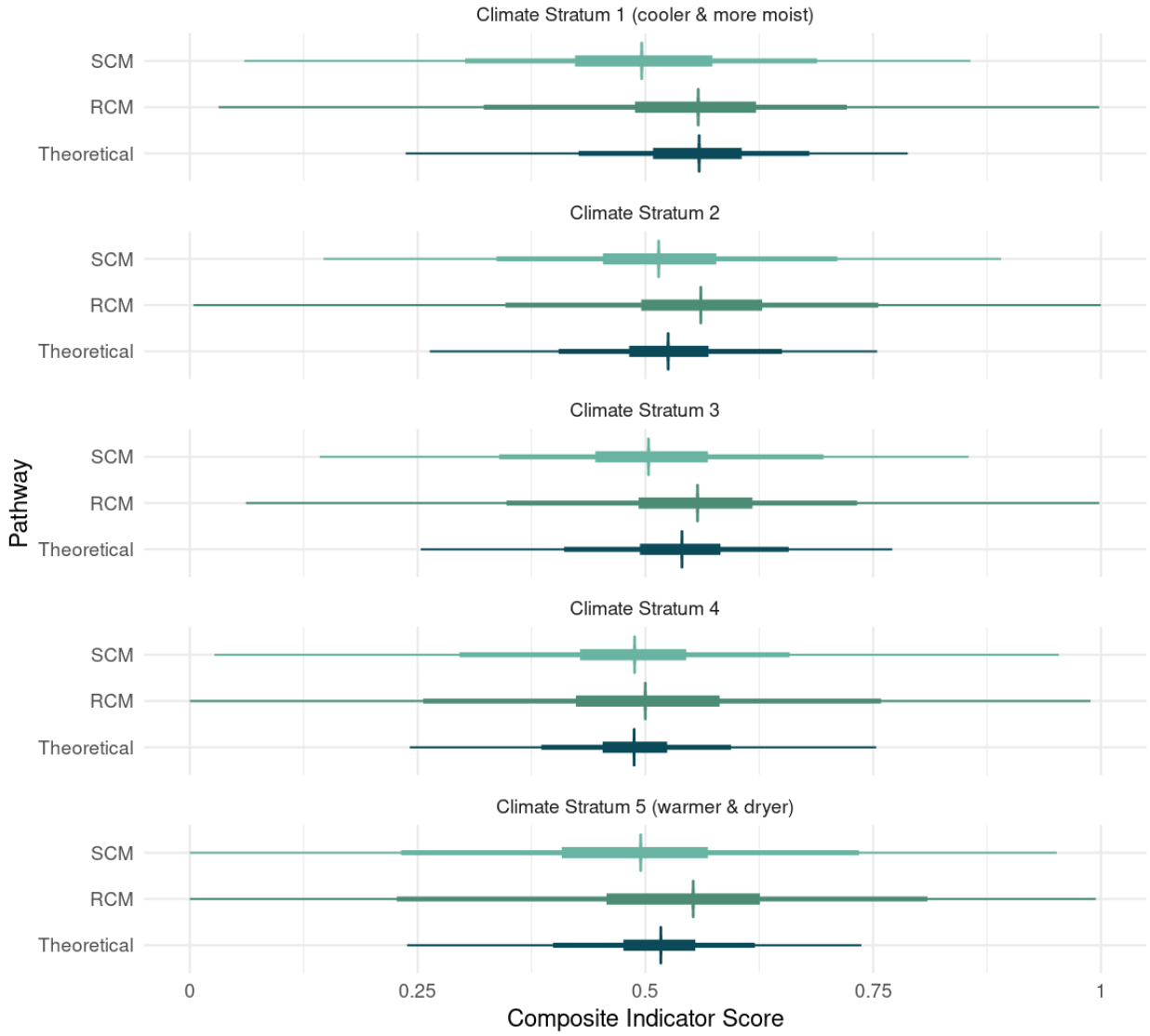

Figure 10: Boxplots showing the statistical distribution of the composite indicator of forest resilience across the Sierra Nevada, California, for each methodological pathway: Theoretical, real core metrics (RCM), and synthetic core metrics (SCM). The statistical distribution is presented for each climate stratum mapped across the landscape.

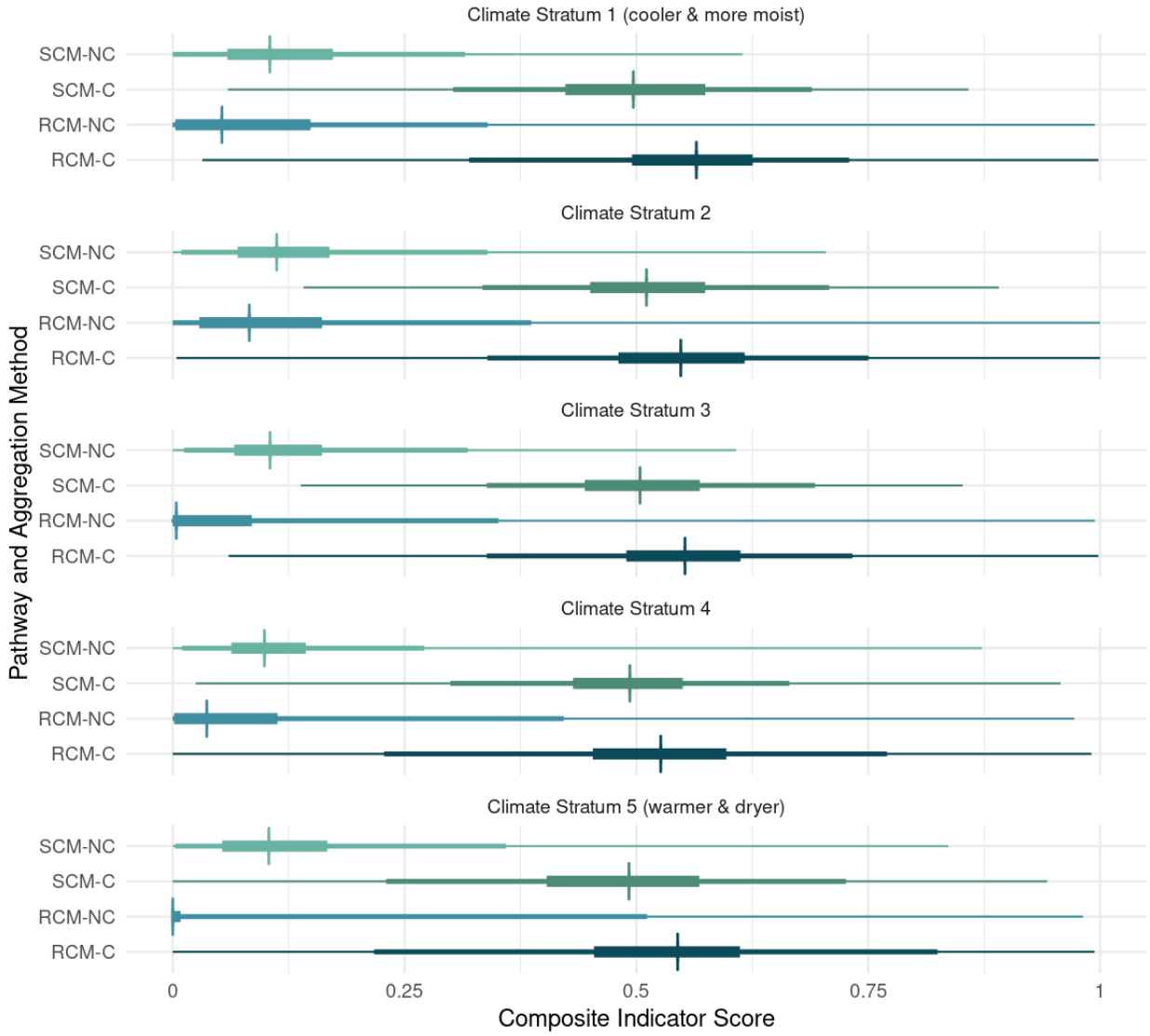

Figure 11: Boxplots showing the statistical distribution of the composite indicator of forest resilience across the Sierra Nevada, California, for the proposed methodological pathways: real core metrics (RCM) and synthetic core metrics (SCM), and based on the aggregation method: compensatory (C) and non-compensatory (NC). The statistical distribution is presented for each climate stratum mapped across the landscape.

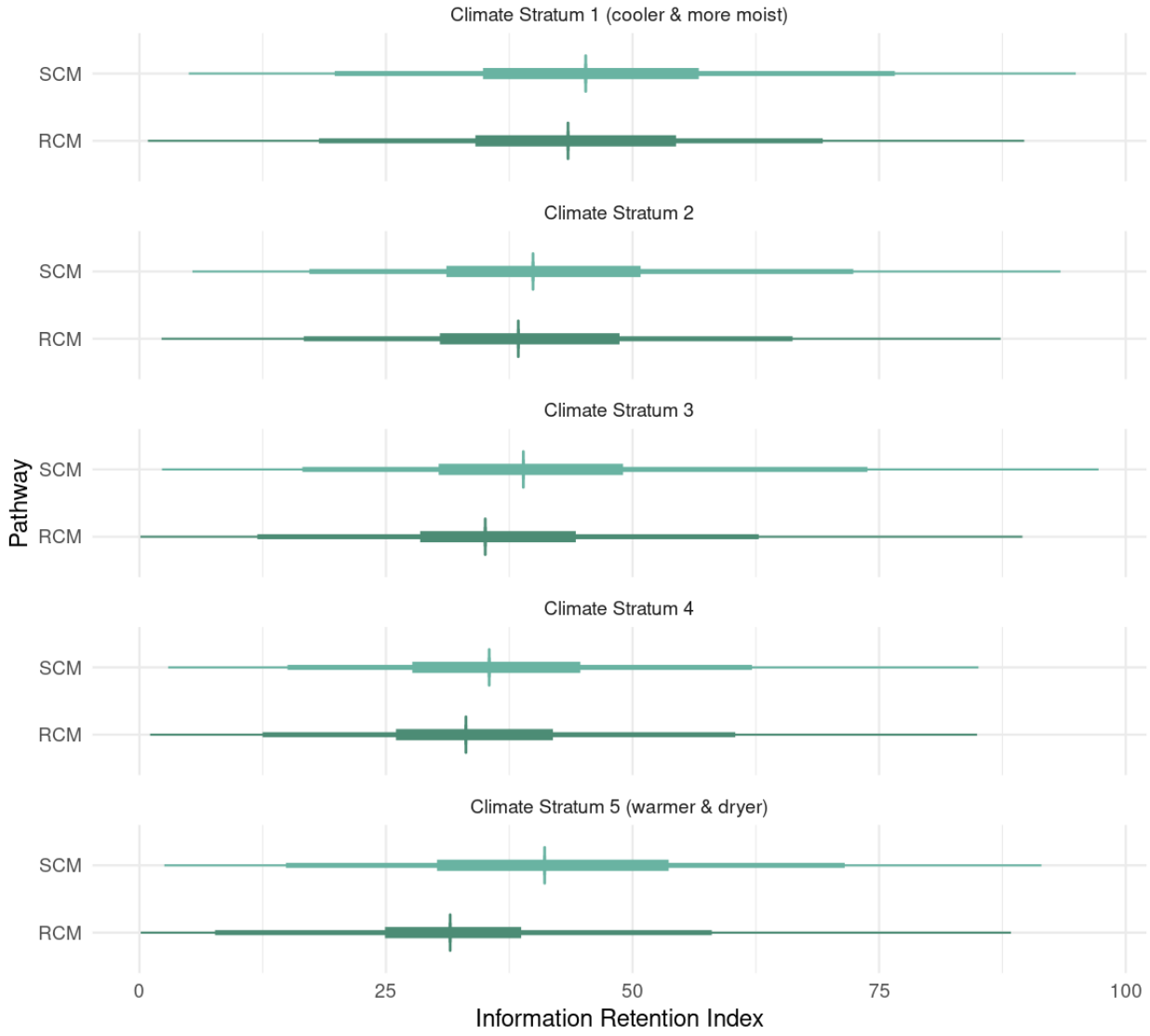

Figure 12: Boxplots showing the statistical distribution of the information retention index (IRI) across the Sierra Nevada, California, for the proposed methodological pathways: real core metrics (RCM), and synthetic core metrics (SCM). The statistical distribution is presented for each climate stratum mapped across the landscape.

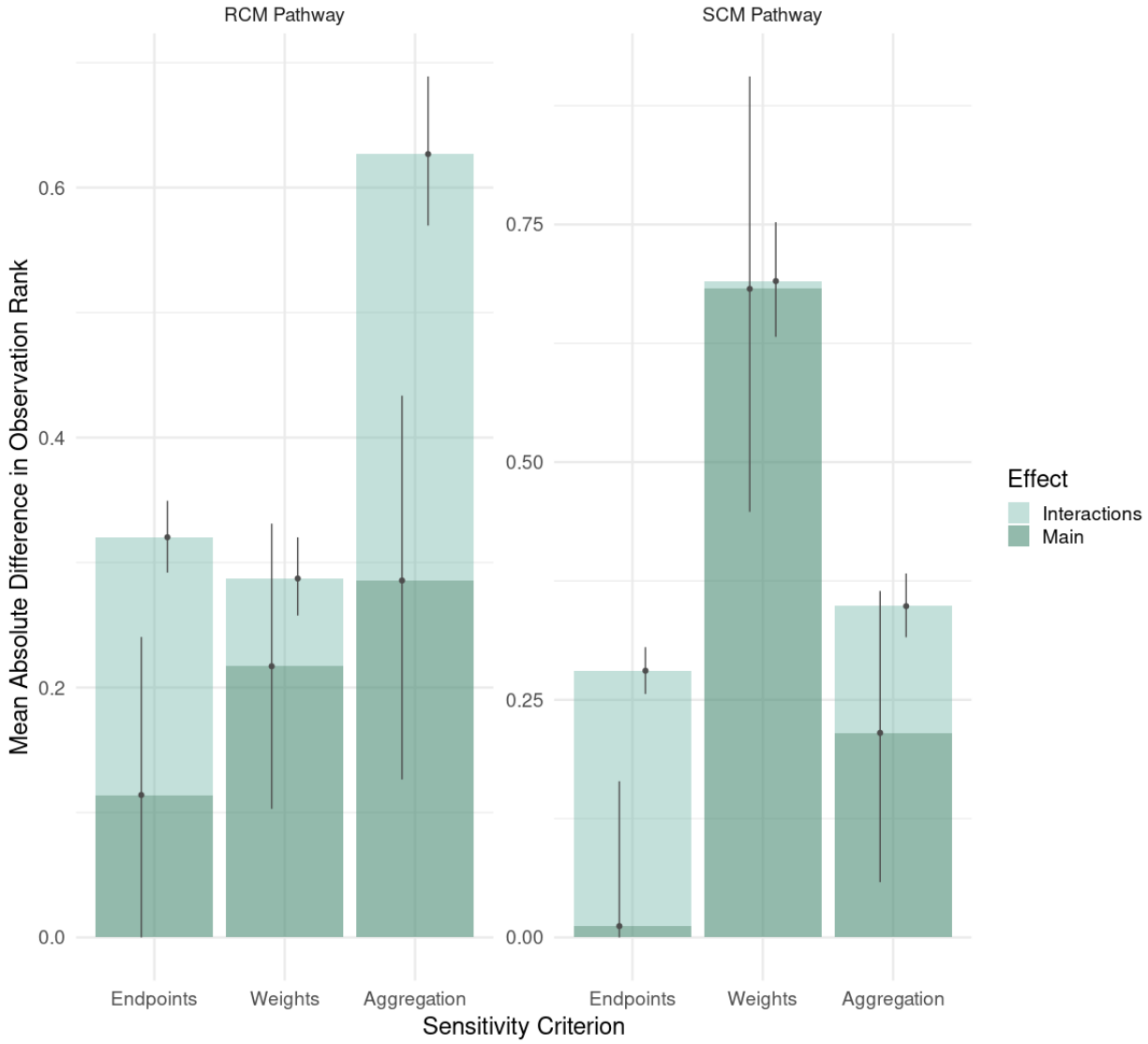

Figure 13: Barplots showing the composite indicator sensitivity index, expressed as the mean absolute difference in data point (i.e., observation) rank by sensitivity criterion (endpoint values, weights, and aggregation method), across the Sierra Nevada, California. Error bars indicate the 5th, 50th, and 95th percentiles. The effect of the sensitivity criterion is assessed as the main effect and as a confounding (i.e., interaction) effect.

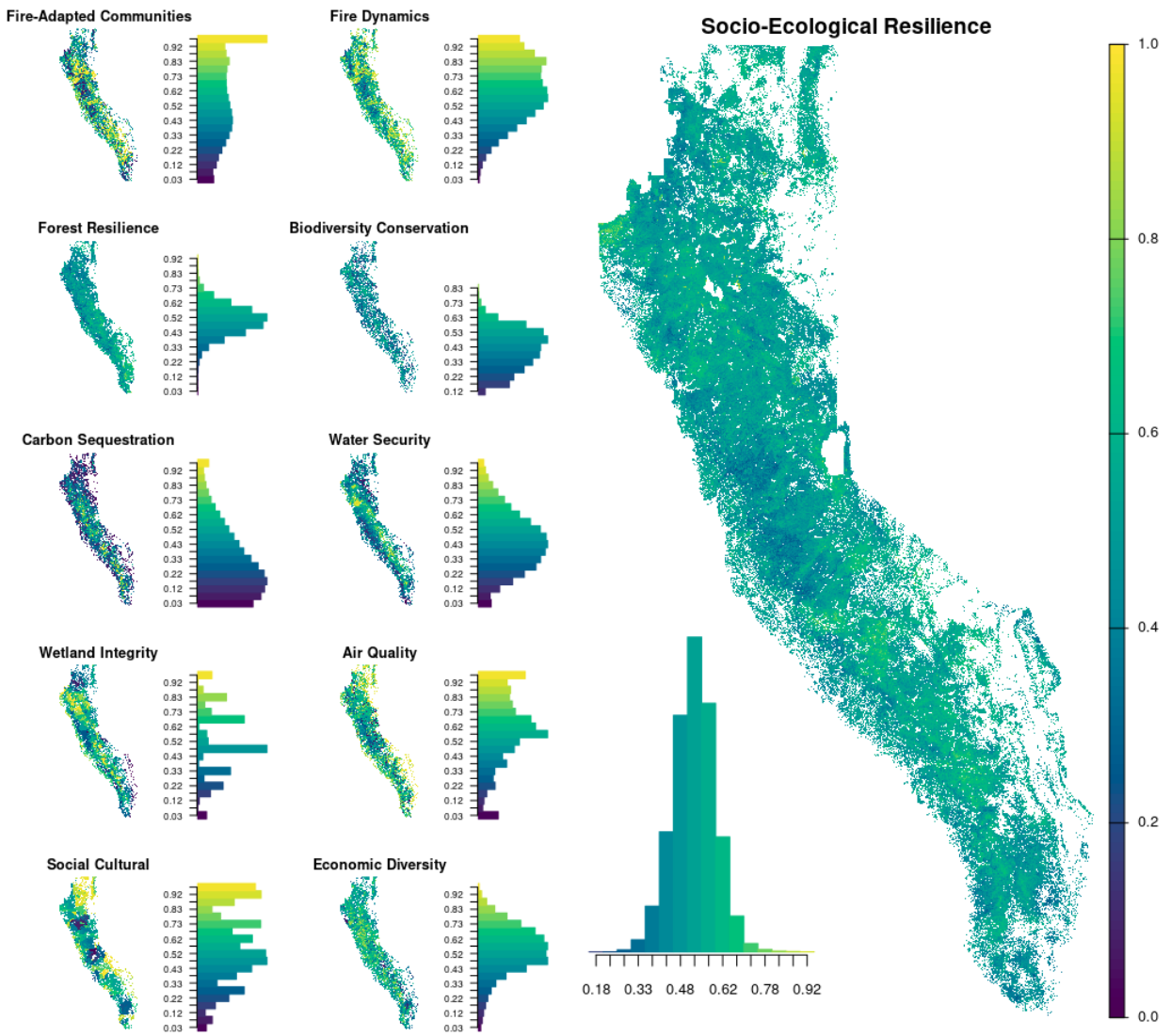

Figure 14: Maps of composite indicator scores for each of the 10 pillars and the overall socio-ecological resilience score across the Sierra Nevada, California.

Table 1: Metrics and elements of the forest resilience pillar as per the Ten Pillars of Resilience (TPOR) Framework (Manley et al., 2023).

Metric	Short Name	Description
Basal Area	BA	The cross-sectional area of tree trunks measured at diameter breast height (dbh). Expressed in square feet per acre.
Tree Density	TPA	The number of trees per acre, commonly used to assess forest structure and habitat condition.
Large-Tree Density	TPA30	The number of large trees, defined as those with diameters at breast height (dbh) >30 inches, per raster pixel.
Stand Density Index	SDI	Relates the current stand density to an equivalent density in a stand with a quadratic mean diameter of 10” (Reineke, 1933).
Canopy Fractal Dimension Index	FDI	A measure of canopy shape complexity, ranging from 1 (simple, continuous canopy) to 2 (highly complex, interrupted canopy).
Early Seral Stage Proportion	eSE	Proportion seedlings (dbh < 1”) and saplings (1” < dbh < 6”) in a stand.
Late Seral Stage Proportion	lSE	Proportion of medium to large trees (dbh > 24”) in a stand.
Large-Snag Density	Snag40	Number of snags per acre from all species and all decay classes with diameters of 40” dbh and greater.
Tree Mortality	Mort	The dead tree canopy cover fraction change between 2017 and 2021, considering insect and disease causes only.
Time Since Last Disturbance	TSD	Time in years before 2021 since the most recent disturbance of at least 25% canopy cover loss per 30m pixel.

Table 1 (cont).

Data Source	Pre-Processing	Element	A Priori Interpretation	Normalization Method
Imputation of FVS runs on FIA plot data (Huang et al., 2018)	Square root transformation	Structure	Lower is better	Negative, piecewise linear slope
Imputation of FVS runs on FIA plot data (Huang et al., 2018)	Logarithmic transformation	Structure	Lower is better	Negative, piecewise linear slope
Imputation of FIA plot data and allometric equations	Logarithmic transformation	Structure	Higher is better	Positive, piecewise linear slope
Imputation of FVS runs on FIA plot data (Huang et al., 2018)	None	Structure	Lower is better	Negative, piecewise linear slope
Canopy height model analysis (Chamberlaing et al., 2023)	Range clamping at percentile 99.5	Structure	Higher is better	Positive, piecewise linear slope
Imputation of FVS runs on FIA plot data (Huang et al., 2018)	None	Composition	Lower is better	Negative, piecewise linear slope
Imputation of FVS runs on FIA plot data (Huang et al., 2018)	None	Composition	Higher is better	Positive, piecewise linear slope
Imputation of FVS runs on FIA plot data (Huang et al., 2018)	Logarithmic transformation	Composition	Higher is better	Positive, piecewise linear slope
Segmented dynamic detection algorithm (Koltunov et al., 2020)	Logarithmic transformation	Disturbance	Lower is better	Negative, piecewise linear slope
Segmented dynamic detection algorithm (Koltunov et al., 2020)	Majority filter (4-cell radius)	Disturbance	Higher is better	Positive, piecewise linear slope

Table 2: Composite variance explained by each of three real core metrics of forest resilience for each of five climate strata across the Sierra Nevada, California, before and after weight optimization, including the final (optimized) weights.

Metric	Stratum	Initial Explained Variance	Optimized Weight	Optimized Explained Variance
SDI	1	0.162	0.375	0.334
	2	0.303	0.340	0.334
	3	0.286	0.348	0.334
	4	0.165	0.420	0.334
	5	0.269	0.390	0.334
eSE	1	0.447	0.306	0.334
	2	0.245	0.357	0.334
	3	0.345	0.330	0.334
	4	0.471	0.260	0.333
	5	0.440	0.304	0.334
Snag40	1	0.391	0.319	0.332
	2	0.451	0.303	0.332
	3	0.369	0.323	0.332
	4	0.363	0.320	0.333
	5	0.469	0.306	0.333

Table 3: Composite variance explained by each of three synthetic core metrics of forest resilience for each of five climate strata across the Sierra Nevada, California, before and after weight optimization, including the final (optimized) weights.

Metric	Stratum	Initial Explained Variance	Optimized Weight	Optimized Explained Variance
SynthMet1	1	0.332	0.334	0.334
	2	0.366	0.315	0.334
	3	0.414	0.295	0.334
	4	0.310	0.342	0.334
	5	0.407	0.235	0.333
SynthMet2	1	0.325	0.338	0.334
	2	0.331	0.339	0.334
	3	0.293	0.355	0.334
	4	0.268	0.361	0.334
	5	0.345	0.354	0.334
SynthMet3	1	0.343	0.329	0.333
	2	0.303	0.347	0.333
	3	0.293	0.350	0.333
	4	0.422	0.296	0.333
	5	0.248	0.411	0.333